Trends in Phytochemical Research (TPR)

Journal Homepage: https://sanad.iau.ir/journal/tpr

Original Research Article

Comparative study of phytochemical composition, oral toxicity, antioxidant, and anticancer activities of both *Aloe vera* and *Aloe vacillans* (Asphodelaceae family) flowers extract: *In vitro*, *in vivo, and in silico studies*

Asma Mohsan Mohammed Al-Wajih[1], Amina El-Shaibany[1], Mahmoud Mahyoob Alburyhi[2], Ahmed S. Abdelkhalek[3], Mahmoud M. Elaasser[4], And Ali E. Raslan[5]*

[1]Pharmacognosy Department, University of Sana'a, Pharmacy College, Sana'a, Yemen
[2]Department of Pharmaceutics and Industrial Pharmacy, Pharmacy College, University of Sana'a, Sana'a, Yemen
[3]Medicinal Chemistry Department, Faculty of Pharmacy, Zagazig University, Zagazig 44519, Egypt
[4]The Regional Center for Mycology and Biotechnology, Al-Azhar University, 11787 Nasr City, Cairo, Egypt
[5]Department of Pharmacognosy, Faculty of Pharmacy, Al-Azhar University, Assiut 71524, Egypt

ABSTRACT

The research study aimed to compare the chemical composition, acute toxicity, antioxidant, and antiproliferative activities of extracts from *Aloe vera* and *Aloe vacillans* flowers. Gas chromatography-mass spectrometry (GC-MS) analysis identified 79 components in the *n*-hexane fraction of *A. vera* flowers (AVeFHF). The toxicity study indicated no mortality or morbidity at the tested concentrations for any of the mice treated with the investigated extracts. *A. vera* flowers methanolic extract (AVeFME) exhibited dose-dependent antioxidant activity. AVeFME demonstrated significant anticancer efficacy against HCT-116, Caco-2, A-549, and RD cell lines, with IC_{50} values of 14.0, 14.6, 12.0, and 14.7 µg/mL, respectively. AVeFHF exhibited moderate anticancer activity against HCT-116, A-549, and RD cell lines. Histological examination revealed substantial morphological changes consistent with the apoptotic mechanism of action. The molecular docking study provided insights into the binding modes of the identified compounds with EGFR and PARP-1 enzymes.

ARTICLE HISTORY

Received: XXX
Revised: XXX
Accepted: XXX
ePublished: XXX

KEYWORDS

Aloe vacillans
Aloe vera
Asphodelaceae family
Anticancer
Antioxidant
Oral toxicity
Phytochemical composition
In vitro
In vivo
In silico

1. Introduction

Cancer is one of the main causes of mortality worldwide, attributed to the excessive division of abnormal cells and caused by several kinds of factors such as chemical mutagens and cancer-causing chemicals (Chan et al., 2011; Konaka et al., 2012; Fathi Karkan et al., 2017; Mahdavi and Mohammadhosseini, 2022). In response, extensive research has been conducted in the past decades to identify various molecular targets that could be exploited for both cancer prevention and treatment (Sak, 2014; Aberoumandi et al., 2017). Typical strategies for therapy include targeting the tumor cells with ionizing radiation, surgical removal of tumor tissue, and chemotherapy. However, current cancer therapy approaches have severe systemic side effects (Bailly, 2021; Arputhaswamy et al., 2024). Therefore, there is an urgent need for more effective cancer therapies with less severe side effects (Reddy et al., 2003). Recent studies have been focused on looking for alternative medicines originating from plant-based sources (Sak, 2014). Traditional and alternative medicines, with their phytochemical components, have long been acknowledged for their significant pharmacological and biological activities and are widely employed in the healthcare maintenance (Mohadjerani and Asadollahi, 2019; Al-Hakami et al., 2024; Dekdouk et al., 2024). For millennia, natural products, particularly those derived from plants, have been employed in the treatment of numerous disorders (Abdollahi-Ghehi et al., 2019). These plant-derived phytochemicals encompass a wide range of compounds such as vitamins, carotenoids, terpenoids, flavonoids, alkaloids, tannins, saponins, enzymes, and minerals. Their inherent antioxidant properties offer the potential for the prevention and treatment of diverse diseases, including cancer (Dixit

Corresponding author: Ali E. Raslan
Tel.: +201003015695; Fax:+201003015695
E-mail address: aliraslan@azhar.edu.eg, **https://doi.org/**

and Ali, 2010). Approximately, 74% of anticancer drugs either originate from natural sources or are inspired by natural products (Newman et al., 2003). Integrating alternative medicines with standard cancer treatments can mitigate side effects (Goldstein, 2003), improve the intake of conventional medicines, and bolster the immune system's capacity to combat cancer. Since these medications are derived from naturally occurring flora extracts, their bioavailability is less likely to trigger severe immune responses (Chan et al., 2011).

The genus *Aloe* is renowned for its extensive history of medicinal applications and is commonly utilized in Chinese and traditional Ayurvedic medicine (Harlev et al., 2012; Mukherjee et al., 2014). For over 2000 years, civilizations including Egypt, Greece, and China have utilized *A. vera* as a drug and food, and its traditional applications encompass addressing constipation, promoting wound healing, and employing it as an anti-tumor remedy (Tong et al., 2021). Several research studies have revealed that *A. vera* has antidiabetic, antibacterial, anticancer, and antiviral effects (Chen et al., 2014; Hussain et al., 2015; Majumder et al., 2019). Over the past couple of decades, basic research has begun to unveil the pharmaceutical potential of *Aloe*, particularly in combating neoplastic diseases. Their anticancer properties are attributed to at least three different mechanisms based on immunostimulatory, antiproliferative, and antioxidant actions (Harlev et al., 2012). The presence of aloe latex (a yellow bitter-tasting component of *A. vera*) is responsible for the antiproliferative activity, while the immuno-stimulatory effect is due to *Aloe* polysaccharides (Lissoni et al., 2009). In southern Yemen's mainland, *A. vacillans* juice has traditionally been employed by local populations to treat malaria (Al-Fatimi, 2023).

The current study aimed to conduct a comparative analysis of the phytochemical profiles, acute oral toxicity, *in vitro* antioxidant activity, and antiproliferative effects of the flowers of *A. vera* (L.) Burm.f. and *A. vacillans* Forssk. (Family: Asphodelaceae). Additionally, a histological examination of treated cancer cells was performed. Furthermore, a molecular docking study was conducted to explore the proposed cytotoxic mechanisms of action for the active compounds.

2. Experimental

2.1. Plant material identification, collection, and preparation

The flowers of *A. vera* (L.) Burm.f. and *A. vacillans* Forssk. were collected from Badaan and Mytam zones in the morning and afternoon, respectively, in Ibb city, Yemen, during 2021/2022. The taxonomic identification of *A. vera* flowers was conducted and authenticated by Dr. Ali Ahmed Abbas Al-Agmi, Department of Biology, Faculty of Education, Dhamar University, Yemen. A. vacillans flowers were identified by Dr. Hassan Ibrahim, Professor of Plant Taxonomy, Botany Section, Department of Biology, Faculty of Science, Sana'a University, Yemen. A voucher specimen (Sa/Phar/Pharm623 and Sa/Phar/Pharm624) was deposited at the Herbarium of Faculty of Pharmacy, Pharmacognosy Department, Sana'a University, Sana'a city, Yemen. The flowers were carefully plucked from the inflorescence, cleaned, divided into small parts, dried away from sunlight and moisture, powdered, weighed, and finely stored in airtight containers at room temperature.

2.2. Extraction and fractionation

The dried powders of *A. vera* (730 g) and *A. vacillans* (1200 g) flowers were macerated in MeOH (3 L x 4). The extract was then filtered and concentrated using a rotary evaporator (Buchi, Switzerland) at a temperature of 45 °C to yield 5 and 20 g of AVeFME and AVaFME. The total extract was then fractionated using different solvents based on their polarity index, starting with *n*-hexane, followed by $CHCl_3$, EtOAc, and finally *n*-BuOH. The fractions were concentrated by using a rotary evaporator and dried using a freeze dryer. The resulting fractions were the *n*-hexane fraction (AVeFHF, 1.4 and AVaFHF 2.7 g), $CHCl_3$ fraction (AVeFCF, 0.8 and AVaFCF 1.8 g), EtOAc fraction (AVeFEF, 1.9 and AVaFEF, 0.8 g), *n*-BuOH fraction (AVeFBF, 1.0 and AVaFBF, 2.7 g), and aqueous fraction (AVeFAF, 1.2 and AVaFAF, 2.0 g), respectively.

2.3. Total phenolic and flavonoid contents assay

The total phenolic and flavonoid contents were quantified using the Folin-Ciocalteu and the $AlCl_3$ colorimetric methods, respectively according to the methods described by (Elkomy et al., 2023). The total phenolic and flavonoid contents were expressed as mg GAE/g extract and mg QE/g extract, respectively.

2.4. GC-MS analysis of phytoconstituents

Identification of AVeFHF compounds was conducted using 1 µL of a 2 mg/mL extract with a Shimadzu GCMS-QP2010 SE system. Helium served as a carrier gas at a flow rate of 1 mL/min, and a fused silica capillary column (30 m × 0.32 mm × 0.10 µm) was employed. The column temperature program commenced at 150 °C for 1 min and increased at a rate of 6 °C/min until it reached 320 °C. The injector and detector temperatures were maintained at 250 °C. Mass spectra were acquired at 70 eV, with scans ranging from 40 to 450 Da at a rate of 2 scans/sec. Compound identification was achieved by comparing the mass spectra with the NIST library and relevant literature data
(Motta et al., 2011).

2.5. Acute oral toxicity study

The acute oral toxicity of AVeFME and AVaFME was assessed in mice following the guidelines of the Organization for Economic Co-operation and Development (OECD) 423. All animal procedures were conducted in accordance with international guidelines for animal care and use and were approved by the

Institutional Ethical Committee, Faculty of Medicine and Health Sciences, Sana'a University, with voucher number (no. 250-3/3/2022). A total of 30 mice, each weighing between 20 and 25 g, were divided into five groups, with six animals per group. The animals were fasted for approximately 12 hours prior to dosing. The 1st (control) group received 10 mL/kg of normal saline, while the 2nd and 3rd groups received gradually increasing oral doses of AVaFME, ranging from 0.1 to 5 g/kg. The fourth and fifth groups received gradually increasing oral doses of AVeFME, also ranging from 0.1 to 5 g/kg. The doses were adjusted based on the body weight of each mouse. The animals were continuously observed for behavioral changes and signs of general toxicity for one hour, and the mortality of mice in each group was recorded 24 hours after the administration of the extracts. All animals were monitored for any signs of physical and behavioral alterations for seven days. At the end of the study, the animals were weighed, and blood samples were collected via cardiac puncture under anesthesia. Serum was then separated for biochemical evaluations (Bello et al., 2016).

2.6. *In vitro* antioxidant assay

The antioxidant activity was assessed using a DPPH free radical scavenging assay conducted in triplicate as follows: a freshly prepared solution of DPPH radical in MeOH (0.004% *w/v*) was stored at 10 °C in the dark. Each tested sample's stock solution was diluted with MeOH and a 40 µL aliquot of the MeOH solution was added to 3 mL of the DPPH solution. Absorbance measurements were taken using a UV-visible spectrophotometer (Milton Roy, Spectronic 1201) after a 30-minute incubation in the dark. The decrease in absorbance at 515 nm was continuously monitored, and absorbance values for the DPPH radical without an antioxidant (control) and the reference compound ascorbic acid were also recorded. Three replicates of each determination were performed and averaged (Mishra et al., 2012; Rehman et al., 2022). The PI (percentage inhibition) of the DPPH radical was calculated according to the following formula (Eqn. 1):

$$PI = (A_{control} - A_{sample}/A_{control}) \times 100 \quad \text{(Eqn. 1)}$$

2.7. Cytotoxic assay

2.7.1. Cell line culture

Various cancer cell lines including HepG-2 (hepatocellular carcinoma), HCT-116 (colon carcinoma), Caco-2 (intestinal carcinoma), A-549 (lung carcinoma), MCF-7 (breast carcinoma), PC-3 (prostate carcinoma), RD (human muscle rhabdomyosarcoma), HEP-2 (larynx carcinoma), HELA (cervical carcinoma), CHO-K1 (ovary carcinoma), and M-NFS-60 (myelogenous leukemia carcinoma) were obtained from the American Type Culture Collection (ATCC, Rockville, MD). Cytotoxicity was assessed using a CVS (crystal violet staining) assay (Elsanhoty et al., 2022). A method developed for evaluating the cytotoxicity of chemicals, following the guidelines of the National Cancer Institute (NIC) and Geran protocols (Geran et al., 1972).

2.7.2. Selectivity index (SI)

To evaluate the cytotoxicity of the extracts against normal cell lines, specifically the MRC-5 cell line was obtained from the American Type Culture Collection (ATCC, Rockville, MD). The degree of selectivity of the product can be expressed by the selective index (SI) value. The SI is calculated as the CC_{50} for the normal cell line/IC_{50} for the cancerous cell line after 48 hours of extract treatment. A high SI value (≥ 2) indicates selective toxicity against cancer cells, while an SI value of < 2 suggests potential toxicity to normal cells (Zorzanelli et al., 2018). Therefore, we assessed AVeFME and AVeFHF for cytotoxicity against the MRC-5 cell line.

2.7.3. Microscopic observation of the tumor cells treated with extract

After treatment with the tested concentrations, the medium was removed, and the wells were washed three times with 300 µL of phosphate-buffered saline (PBS) at pH 7.2. The cells were then fixed to the plate using 10% formalin for 15 min at room temperature. Subsequently, the fixed cells were stained with 100 µL of crystal violet (0.25%) for 20 min. Any excess stain was removed by rinsing the plates with deionized water, and the plates were allowed to dry. An inverted microscope (CKX41; Olympus, Japan) equipped with a digital microscopy camera was used to capture images that represented the morphological changes compared to control cells. The cytopathic effects (morphological alterations) were microscopically observed at 100× magnification (Amin et al., 2018).

2.7.4. Annexin V-FITC/PI dual staining and cell cycle analysis

The propidium iodide staining, followed by flow cytometric analysis, was performed using the cell cycle kit (ab139418) to investigate the effect of *Aloe vera* extract on the phases of the cell cycle. To detect apoptosis in the treated cells, the Annexin V-FITC apoptosis detection kit (K101-25, Biovision, USA) was utilized, followed by flow cytometric analysis in accordance with the manufacturer's protocol.

2.7.5. Molecular docking

The crystal structures of PARP-1 (PDB ID: 5DS3) and EGFR (PDB ID: 2RGP) were obtained from the Protein Data Bank (https://www.rcsb.org). The QuickPrep protocol was utilized for target preparation. The 3D structures of the compounds were generated using 2D structures retrieved from the PubChem database (as SMILES) using the Molecular Operating Environment (MOE 2019.0102, Chemical Computing Group Inc., Montreal, Quebec, Canada). This process was followed by energy minimization and protonation. Finally, the docking module was employed in the docking studies,

with all other related parameters set to their default values. Pose selection was based on the S-value, root mean square deviation (RMSD), and pose visualization. The docking protocol was validated by redocking the co-crystallized compounds at 2WXG and 2RGP, respectively.

2.8. Statistical analysis

All data were analyzed by using Graph Pad Prism software version 8 (Graph Pad Software, Inc., CA, USA); $p < 0.05$, $p < 0.01$, and $p < 0.001$ values are considered significant. Statistical analysis was performed using ordinary one-way and two-way ANOVA followed by Dunnett's or Tukey's post hoc tests to perform pairwise comparisons between the groups to identify which specific group(s) exhibit significant differences. Statistical significance was indicated by p-values < 0.001, < 0.01, and < 0.05.

3. Results and Discussion

3.1. Phytochemical composition

The phytochemical analysis revealed that AVFaME contained several groups of phytochemical constituents, including flavonoids, phenolic compounds, carbohydrates, proteins, and sterols. On the other hand, AVFeME demonstrated the presence of carbohydrates, saponins, flavonoids, steroids, proteins, and phenolic compounds (Table 1). The phytochemical composition of AVFeME was previously detailed via UHPLC-Q/Orbitrap/MS/MS. This analysis identified sixteen phenolic compounds, including chlorogenic acid, caffeic acid, 5-feruloylquinic acid, aloesin (or aloeresin B), aloe emodin-diglucoside, orientin, isoquercitrin, chrysoeriol-7-*O*-glucuronide, kaempferol-3-O-hexosyl-*O*-pentoside, kaempferol, 10-hydroxyaloin A, aloin A, isovitexin, isoaloeresin D, 6′-malonyl aloin, aloe emodin-8-*O*-glucoside, and eupatorin, along with an oxylipin identified as trihydroxy octadecenoic acid (Quispe et al., 2018). In another study, seventeen phenolic compounds were identified and quantified using RP-HPLC, yielding kaempferol, quercitrin, apigenin, rutin, myricetin, catechin, epicatechin, sinapic acid, chlorogenic acid, protocatechuic acid, syringic acid, vanillic acid, gallic acid, gentisic acid, caffeic acid, *p*-coumaric acid, and ferulic acid (López et al., 2013). HPLC-DAD and HPLC-MS/MS analyses confirmed the presence of caffeic acid, 5-*p*-coumaroylquinic acid, chlorogenic acid, caffeoyl shikimic acid, 5-feruloylquinic acid, ferulic acid, *p*-coumaric acid, isovitexin, and isoorientin (Keyhanian and Stahl-Biskup, 2007).

3.2. Total phenolics and flavonoids contents

It can be observed that AVeFME exhibited a higher content of phenolic compounds, measuring 150.44 ± 4.62 mg GAE/g dry extract, compared to AVaFME, which had 98.07 ± 5.89 mg GAE/g dry extract. In contrast, AVeFHF displayed a relatively lower phenolic content of 46.35 ± 5.35 mg GAE/g dry extract. Furthermore, AVaFME demonstrated a higher flavonoid content of 94.71 ± 1.02 mg QE/g dry extract compared to AVeFME, which had 70.38 ± 0.97 mg QE/g dry extract. Meanwhile, AVeFHF showed a lower flavonoid content of 28.39 ± 1.08 mg QE/g dry extract (Table 2). The TPC and TFC of AVeFME were previously studied and reported in our earlier research (Elkomy et al., 2023).

3.3. GC-MS profiling of AVeFME

The study of AVeFME using gas chromatography-mass spectrometry (GC-MS) identified 79 compounds, of which 16 were classified as the main compounds. The most abundant compounds included myristic acid isopropyl ester (37.33%), benzyl benzoate (9.79%), hexadecanoic acid methyl ester (4.13%), stigmast-5-en-3-ol (2.81%), methyl stearate (2.28%), hexadecanoic acid (2.18%), hexadecanoic acid ethyl ester (2.02%), octacosanol (1.80%), linoleic acid ethyl ester (1.53%), stearic acid (1.43%), glycidyl palmitate (1.28%), bis(2-ethylhexyl) phthalate (1.10%), 9,12-octadecadienoic acid methyl ester (1.07%), 9,12,15-octadecatrienoic acid ethyl ester (1.06%), stearic acid ethyl ester (0.98%), stigmast-4-en-3-one (0.67%), 9,12,15-octadecatrienoic acid methyl ester (0.64%), and campesterol (0.61%) (see Table 3, Fig. 1 and Fig. 2).

3.4. Oral toxicity studies protocols

3.4.1. Effect of treatment on behavioral changes

Various parameters were observed and recorded during the investigation, including skin and fur condition, eye appearance, respiration, salivation, urination, fecal consistency, somatomotor activity and behavioral patterns, mucous membrane status, convulsions and tremors, itching, sleep patterns, coma, and mortality. Notably, no morbidity or mortality was detected in any of the mice treated with the studied extracts. Furthermore, no signs of acute toxicity, such as diarrhea, hematuria, restlessness, uncoordinated muscular movements, or respiratory distress, were observed. However, the administration of AVaFME at dosages exceeding 3 g/kg b.w. resulted in some toxicity within the tested group throughout the entire observation period (Table 4). Consequently, the LD_{50} for this extract is estimated to be greater than 3 g/kg b.w. In contrast, AVeFME was deemed safe at doses below 5 g/kg b.w. suggesting an estimated LD_{50} exceeding 5 g/kg b.w.

3.4.2. Effect of AVeFME and AVaFME on biochemical markers in the acute toxicity study

At a dose of 3 g/kg, both AVeFME and AVaFME exhibited significantly elevated levels of AST and ALT compared to the control group. At 1 g/kg, both extracts also demonstrated statistically significant increases in AST and ALT levels relative to the control group. Notably, at 500 mg/kg, the AST level in the AVaFME group was significantly lower than that of the control group; however, there were no significant differences in AST and ALT levels

Table 1
Phytochemical tests of AVaFME and AVeFME.

Phytochemical constituents	AVaFME	AVeFME
Alkaloids	–ve	–ve
Carbohydrates	+ve	+ve
Glycoside	–ve	–ve
Saponin	–ve	+ve
Flavonoids	+ve	+ve
Steroids	+ve	+ve
Phenolic compound	+ve	+ve
Protein	+ve	+ve
Fixed oils and Fats	–ve	–ve

AVaFME: *A. vacillans* flowers methanolic extract; AVeFME: *A. vera* flowers methanolic extract.

Table 2
The total phenolic and flavonoid contents of AVeFME, AVaFME, and AVeFHF.

Extract	Total phenolic content				Total flavonoid content			
	mg GAE/g dry extract wt.				mg QE/g dry extract wt.			
	S1	S2	S3	Mean ± SD	S1	S2	S3	Mean ± SD
AVaFME	104.71	96.04	93.46	98.07 ± 5.89***	93.62	94.87	95.65	94.71 ± 1.02***
AVeFME	146.78	148.91	155.64	150.44 ± 4.62***	71.26	69.34	70.53	70.38 ± 0.97***
AVeFHF	51.39	40.73	46.92	46.35 ± 5.35***	29.05	27.14	28.97	28.39 ± 1.08***

S1-S3: Extract samples; GAE: Gallic acid equivalents; QE: Quercetin equivalents; wt.: weight; SD: Standard division; AVaFME: *A. vacillans* flowers methanolic extract; AVeFME: *A. vera* flowers methanolic extract; AVeFHF: *n*-Hexane fraction of *A. vera* flowers extract; ***p-value < 0.001.

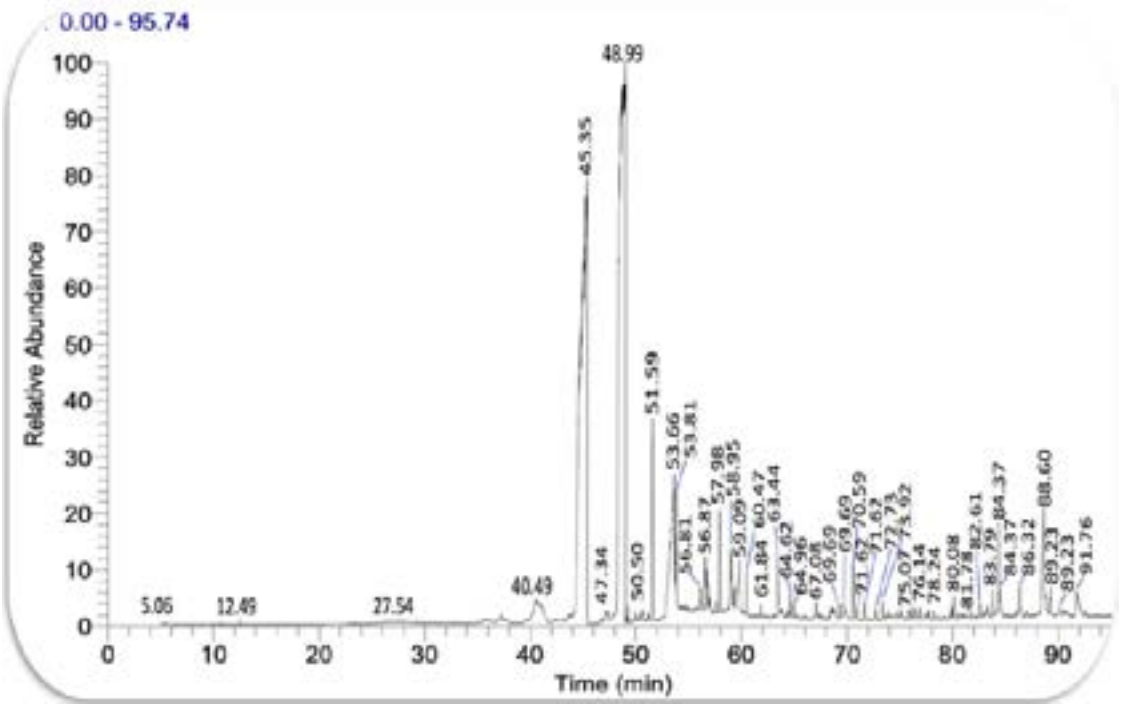

Fig. 1. GC-MS chromatogram for the AVeFME.

Table 3
Phytocomponents identified in the AVeFME by GC-MS.

No.	tR (min)	Compound	SI	RSI	CID	MW	%RC
1	12.49	3-Methyl-2-butenoic acid cyclobutyl ester	745	891	557813	154	0.09
2	40.49	Caryophylla-4(12),8(13)-dien-5-ol	742	781	91753606	220	0.27
3	41.1	5-(1-Isopropenyl-4,5-dimethylbicyclo[4.3.0]nonan-5-yl)-3-methyl-2-pentenol acetate	712	736	5375240	332	0.13
4	43.72	1,8-Di(4-nitrophenylmethyl)-3,6-diazahomoadamantan-9-one	576	640	547088	436	0.11
5	45.35	Benzyl benzoate	946	960	2345	212	9.79
6	47.34	Tetradecanoic acid ethyl ester	657	705	31283	256	0.16
7	48.99	Myristic acid isopropyl ester	938	940	8042	270	37.33
8	49.29	Neophytadiene	845	921	10446	278	0.24
9	49.94	Ethyl iso-allocholate	603	647	6452096	436	0.22
10	50.5	Ethanol, 2-(9-octadecenyloxy)-, (Z)	733	752	5364713	312	0.16
11	50.64	Octadecanoic acid 3-oxo-methyl ester	769	800	84501	312	0.26
12	51.15	Z-(13,14-Epoxy)tetradec-11-en-1-ol acetate	737	757	5363633	286	0.14
13	51.59	Hexadecanoic acid methyl ester	928	929	8181	270	4.13
14	53.66	Hexadecanoic acid	938	948	985	256	2.18
15	53.81	Hexadecanoic acid ethyl ester	895	896	12366	284	2.02
16	56.1	Oleic acid (9-octadecenoic acid)	775	807	445639	282	0.41
17	56.58	9,12-Octadecadienoic acid methyl ester	854	917	8203	294	1.07
18	56.68	9,12,15-Octadecatrienoic acid methyl ester	812	840	5319706	292	0.64
19	56.87	11-Octadecenoic acid methyl ester	813	825	74738	296	0.42
20	57.04	Dasycarpidan-1-methanol, acetate	744	753	550072	326	0.25
21	57.57	Hexadecanoic acid, 2,3-dihydroxypropyl ester	767	768	14900	330	0.24
22	57.95	Methyl stearate	906	969	8201	298	2.28
23	58.95	Linoleic acid ethyl ester	879	919	5282184	308	1.53
24	59.09	9,12,15-Octadecatrienoic acid ethyl ester	867	919	6371716	306	1.06
25	29.28	Ethyl oleate	841	867	5363269	310	0.4
26	59.82	Stearic acid	894	916	5281	284	1.43
27	60.47	Stearic acid ethyl ester	876	877	8122	312	0.98
28	61.84	Hexadecanoic acid, 2-hydroxy-1-(hydroxymethyl)ethyl ester	770	825	123409	330	0.28
29	63.44	Glycidyl palmitate	847	896	347736	312	1.28
30	63.78	Palmitic acid, 2-(tetradecyloxy)ethyl ester	679	712	545600	496	0.17
31	63.89	Hexadecanoic acid, 1-(hydroxymethyl)-1,2-ethanediyl ester	679	683	99931	568	0.12
32	64.42	2H-pyran-2-one-tetrahydro-6-tridecyl	765	818	518573	282	0.15
33	64.62	Docosane	815	826	12405	310	0.53
34	64.96	Methyl icosanoate	785	844	14259	326	0.24
35	67.08	Eicosanoic acid ethyl ester	697	776	537294	340	0.36
36	67.36	2-Monoolein (2-Oleoylglycerol)	765	816	5319879	356	0.09
37	67.7	Dotriacontane	715	762	11008	256	0.08
38	68.31	2-Monostearin (2-Monostearoylglycerol)	736	780	79075	358	0.14
39	68.53	Glyceryl monolinolenate	772	809	5367328	352	0.24
40	68.65	Butyl 9,12,15-octadecatrienoate	752	834	5743460	334	0.23
41	68.77	Glycidyl oleate	787	835	5354568	338	0.13
42	69.29	3-Hydroxypropyl palmitate	665	725	24802448	314	0.29

Table 3
Continued

No.	tR (min)	Compound	SI	RSI	CID	MW	%RC
43	69.69	Glycidol stearate	752	759	62642	340	0.31
44	70.59	Bis(2-ethylhexyl) phthalate	769	848	8343	390	1.1
45	70.93	Docosanoic acid methyl ester	799	835	13584	354	0.27
46	71.62	Benzyl palWmitate	819	926	13908925	346	0.32
47	72.73	Docosanoic acid ethyl ester	763	846	22199	368	0.23
48	73.92	Methyl glycocholate, 3TMS derivative	642	662	22214169	695	0.15
49	74.33	Isochiapin B	687	703	-	346	0.1
50	74.74	1,25-Dihydroxyvitamin D3, TMS derivative	603	649	5364601	488	0.13
51	75.07	1-Hexadecanol, 2-methyl	712	766	17218	256	0.19
52	75.81	Celidoniol, deoxy	763	775	12409	408	0.19
53	76.14	Tetracosanoic acid methyl ester	762	813	75546	382	0.24
54	76.46	13-Docosenamide	734	779	5365369	337	0.22
55	76.93	Benzyl myristate	732	870	3015540	318	0.21
56	77.53	3′,4′,7-Trimethylquercetin	651	664	5280682	344	0.11
57	77.75	Pentacosanoic acid methyl ester	651	679	41431	396	0.16
58	78.24	Dihydroxanthin	604	687	536922	308	0.19
59	79.88	Erucic acid (13-docosenoic acid)	719	770	5281116	338	0.19
60	80.08	Nonacosanol	771	810	243696	424	0.42
61	81.04	1-Heptatriacotanol	689	764	537071	537	0.08
62	81.78	Campesteryl acetate	717	828	13019955	442	0.12
63	82.61	α-Tocopherol	734	769	14985	430	0.32
64	82.61	β-Tocopherol	737	781	6857447	416	0.32
65	82.61	γ-Tocopherol	731	794	92729	416	0.32
66	83.3	Cholesta-4,6-dien-3-ol	679	806	53996943	384	0.22
67	83.79	Stigmast-5-en-3-ol, oleate	749	767	20831071	679	0.57
68	84.37	Octacosanol	866	902	68406	410	1.8
69	84.51	17-Pentatriacontene	793	835	5365022	490	0.24
70	86.07	24-Methylenecholesterol	711	783	92113	398	0.1
71	86.32	Campesterol	842	858	173183	400	0.61
72	88.6	Stigmast-5-en-3-ol	859	866	22012	414	2.81
73	88.82	29-Methylisofucosterol	718	775	6443745	426	0.18
74	89.23	Cycloeucalenol acetate	773	833	537081	468	0.45
75	90.14	Tricyclo[20.8.0.0(7,16)]triacontane, 1(22),7(16)-diepoxy	692	783	543764	444	0.14
76	90.55	Stigmasta-3,5-dien-7-one	678	791	12444466	410	0.12
77	91.76	Stigmast-4-en-3-one	780	873	5484202	412	0.67
78	92.55	Lucenin-2	674	678	442615	610	0.11

t_R, Retention time; SI, Direct matching factors; RSI, Reverse search matching; CID, PubChem's compound identifier; MW, Molecular weight; MF, Molecular formula; % RC, % of Relative concentration.

for either extract when compared to the control group. Additionally, serum creatinine levels were significantly higher in both extracts at dosages of 1 and 3 g/kg compared to the control group, but no significant differences in serum creatinine levels were observed for either extract at a dose of 500 mg/kg. Furthermore, at a dose of 3 g/kg, serum urea levels were significantly higher in the AVaFME group compared to the control group, while no significant differences in serum urea levels were noted at dosages of 500 mg/kg or 1 g/kg when compared to the control group (Table 5).

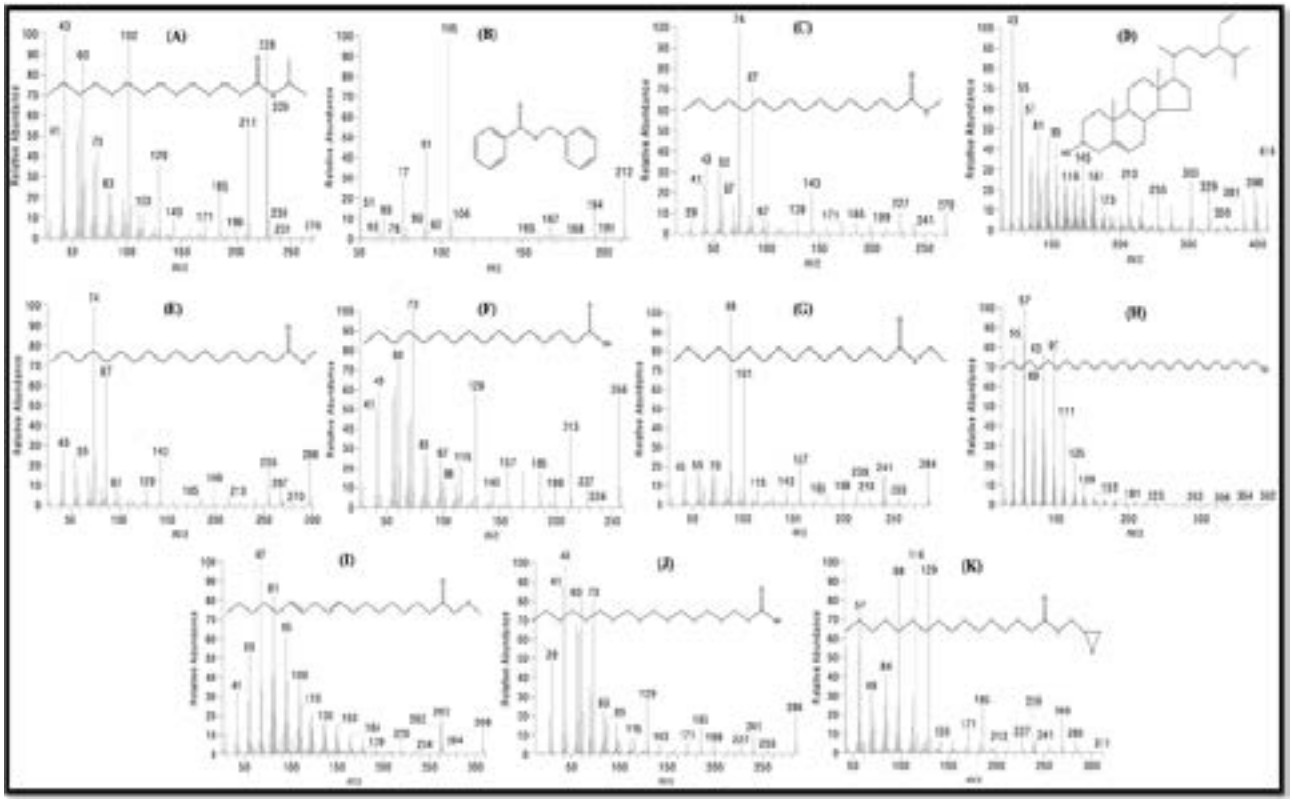

Fig. 2. Mass spectrum of the major compounds identified in AVeFME: (**A**) myristic acid isopropyl ester, t_R = 48.99; (**B**) benzyl benzoate, t_R = 45.35; (**C**) hexadecanoic acid methyl ester, t_R = 51.59; (**D**) stigmast-5-en-3-ol, t_R = 88.60; (**E**) methyl stearate, t_R = 57.95; (**F**) hexadecanoic acid, t_R = 53.66; (**G**) hexadecanoic acid ethyl ester, t_R = 53.81; (**H**) octacosanol, t_R = 84.37; (**I**) linoleic acid ethyl ester, t_R = 58.95; (**J**) stearic acid, t_R = 59.82; (**K**) glycidyl palmitate, t_R = 63.44.

Table 4
Behavioral patterns of AVaFME at dose 3 g/kg and vehicle-treated groups on behavioral changes of mice.

Parameters	Observations of vehicle control and plant extract treated groups									
	30 min		4 h		24 h		48 h		7 Days	
	CG	TG	CG	TG	CG	TG	CG	TG	CG	TG
Fur & skin	N	N	N	N	N	N	N	N	N	N
Eyes	N	Pale reddish	N	N	N	N	N	N	N	N
Respiration	N	Disturbed	N	N	N	N	N	N	N	N
Salivation	N	N	N	N	N	N	N	N	N	N
Urination	N	N	N	N	N	N	N	N	N	N
Faeces consistency	N	N	N	N	N	N	N	N	N	N
Somatomotor activity & behavior pattern	N	N	N	N	N	N	N	N	N	N
Mucous membrane	N	N	N	N	N	N	N	N	N	N
Convulsions and tremors	N	N	N	N	N	N	N	N	N	N
Itching	N	N	N	N	N	N	N	N	N	N
Sleep	N	N	N	N	N	N	N	N	N	N
Coma	N	N	N	N	N	N	N	N	N	N
Mortality	0/6	0/6	0/6	0/6	0/6	0/6	0/6	0/6	0/6	0/6

CG, vehicle control group; TG, AVaFME treated groups; N: not observed.

Table 5

Biochemical analysis of the treated groups in the acute toxicity study.

Sample	Concentration	Liver function test		Renal function test	
		ALT (U/L)	AST (U/L)	Creatinine (mg/dL)	Urea (mg/dL)
AVeFME	3 g/kg	70.70 ± 8.12***	397.42 ± 86.47***	0.43 ± 0.05	38.33 ± 5.50
AVaFME	3 g/kg	75.47 ± 9.72***	342.52 ± 61.86***	0.44 ± 0.08	41.50 ± 3.83
AVeFME	1 g/kg	36.95 ± 4.22	86.52 ± 11.71	0.39 ± 0.03	36.33 ± 2.16
AVaFME	1 g/kg	38.03 ± 3.83	83.45 ± 10.38	0.39 ± 0.03	38.00 ± 3.74
AVeFME	500 mg/kg	28.47 ± 1.21	67.18 ± 2.62	0.34 ± 0.04	34.67 ± 2.42
AVaFME	500 mg/kg	28.08 ± 1.81	58.78 ± 4.14	0.34 ± 0.03	34.00 ± 2.83
Control	-	29.22 ± 3.87	65.03 ± 10.03	0.31 ± 0.07	35.83 ± 4.07

ALT, Alanine transaminase enzyme; AST, Aspartate transaminase enzyme; AVeFME, *A. vera* flowers methanolic extract; AVaFME, *A. vacillans* flowers methanolic extract; ***p-value < 0.001 compared to control.

3.5. *In vitro* antioxidant activity results

The IC_{50} values for AVeFME and AVaFME were determined to be 38.09 ± 4.27 and 176.7 ± 3.59 µg/mL, respectively (Fig. 3). In comparison, the reference compound, ascorbic acid, exhibited an IC_{50} value of 15.01 ± 4.85 µg/mL. These results indicate that the antioxidant activity of AVeFME is significantly stronger than that of the reference ascorbic acid. On the other hand, the antioxidant activity of AVaFME is relatively weak when compared to ascorbic acid (Fig. 3). Our previous study (Elkomy et al., 2023) demonstrated that AVeFME possesses good antioxidant activity compared to ascorbic acid as a reference standard. The results for AVeFME exceed those reported in earlier studies regarding free radical scavenging activity (Keyhanian and Stahl-Biskup, 2007; López et al., 2013; Elkomy et al., 2023).

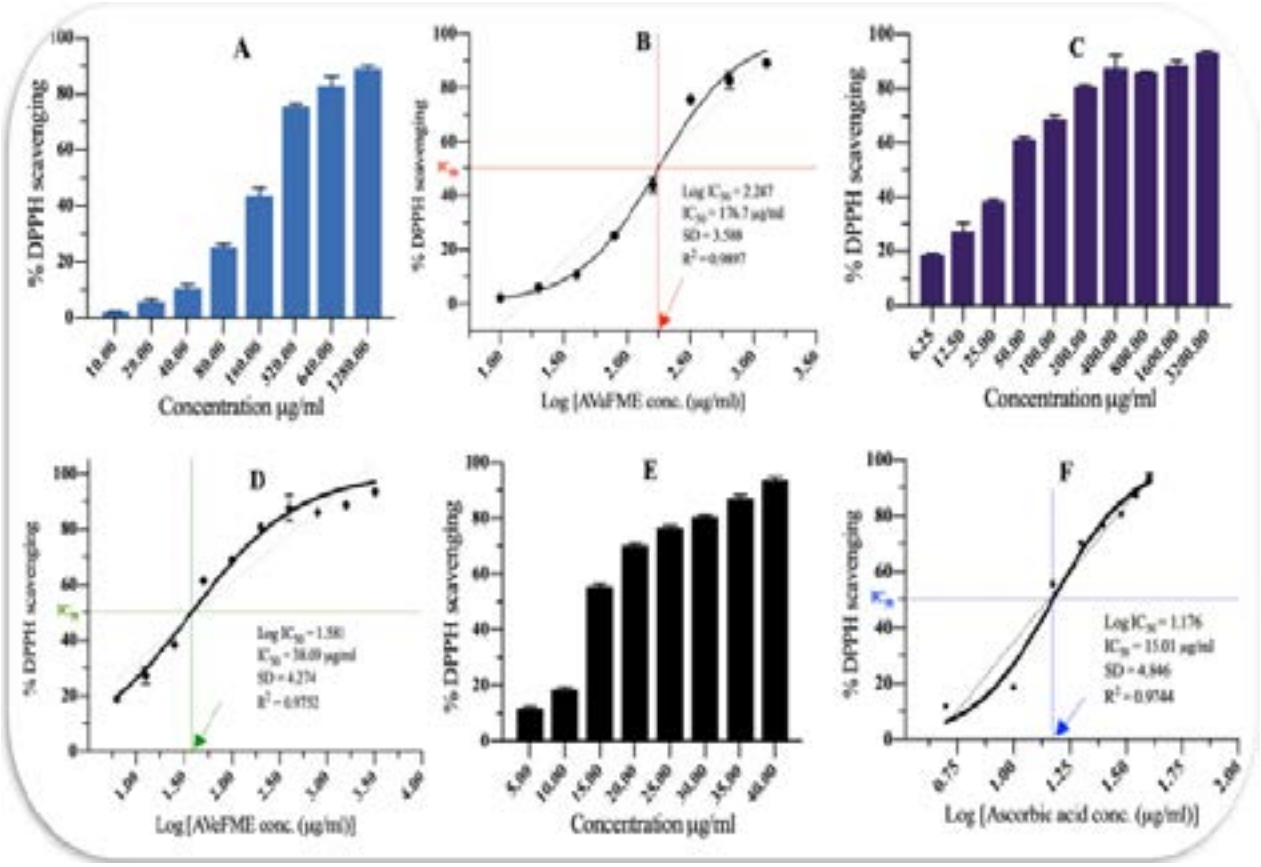

Fig. 3. Antioxidant activity of AVaFME (**A**, **B**), AVeFME (**C**, **D**), and ascorbic acid standard (**E**, **F**) using DPPH scavenging: **A**, **C**, **E**) % of inhibition of free radicals; **B**, **D**, **F**) IC_{50} graph showed IC_{50} derivation from the log concentration-response curve obtained by GraphPad Prism 8 and the value is expressed as mean ± SD.

3.6. Cytotoxic assay

3.6.1. Cytotoxic activity of AVeFME and AVaFME against different cell lines

To evaluate the cytotoxic activity, various cell lines were treated with different concentrations of AVeFME and AVaFME extracts, ranging from 3.9 to 500 µg/mL. The data indicated that some extracts exhibited cytotoxic effects in a concentration-dependent manner, as evidenced by the decrease in cell viability (Fig. 4). AVeFME demonstrated promising cytotoxic activity against the HCT-116, Caco-2, A549, and RD cancer cell lines when compared to the standard vinblastine. According to the guidelines established by the National Cancer Institute (NCI), a crude extract is considered promising if it exhibits IC_{50} values lower than 30 µg/mL after 24 h of exposure. In the case of AVeFME, IC_{50} values below this stringent criterion were observed in four cancer cell lines. The lowest IC_{50} values were recorded for HCT-116 (15.31 ± 3.56 µg/mL), Caco-2 (17.58 ± 3.30 µg/mL), A549 (12.02 ± 2.81 µg/mL), and RD (18.98 ± 4.41 µg/mL) (Table 6). Both *in vitro* and *in vivo* studies have shown that *A. vera* extract contains bioactive compounds such as aloin, aloe-emodin, and aloesin, which have the potential to effectively inhibit cancer cell proliferation (Liu et al., 2012; Majumder et al., 2019; Majumder et al., 2020).

3.6.2. Cytotoxic activity of *A. vera* flowers fractions on HCT-116, Caco-2, A549, and RD cells lines

The cytotoxic properties of various fractions of *A. vera* flowers were evaluated on HCT-116, Caco-2, A549, and RD cell lines (Fig. 5). Among all the fractions tested, AVeFHF exhibited activity against HCT-116, A549, and RD cell lines. When comparing the cytotoxic activity of AVeFHF to the standard vinblastine, statistically significant higher values were observed in the A549 and RD cell lines. Additionally, HCT-116 and Caco-2 also demonstrated statistically significant activity compared to vinblastine. These results indicate that AVeFHF possesses cytotoxic properties and shows promising activity against the tested cell lines, while the other fractions did not exhibit significant cytotoxic effects. The IC_{50} values further confirmed that AVeFHF displayed substantial cytotoxic activity against the cancer cell lines tested. The IC_{50} values obtained for AVeFHF against HCT-116, Caco-2, A549, and RD were 19.33 ± 2.04, 59.79 ± 3.75, 34.14 ± 3.98, and 27.33 ± 3.33, respectively (Table 7).

3.6.3. Selectivity of cytotoxic effect of AVeFME and AVeFHF *vs.* vinblastine standard

AVeFME and AVeFHF did not demonstrate a significant effect on the tested human lung fibroblast cell line (MRC-5). The viability of MRC-5 cells treated with higher concentrations of AVeFME or AVeFHF was reduced, with AVeFHF exhibiting greater toxicity than AVeFME (Fig. 6). The CC_{50} values for AVeFME and AVeFHF were 244.17 and 188.38 µg/mL, respectively, against MRC-5, while the standard vinblastine had a CC_{50} value of 14.03 µg/mL (Table 8). The SI values, which represent the ratio of the CC_{50} value to the IC_{50} value, were calculated and summarized in Table 8. Notably, AVeFME and AVeFHF exhibited higher SI values for the tested cancer cell lines, significantly surpassing that of vinblastine. A higher SI value indicates more promising selectivity properties of a compound, whereas an SI below 2.0 suggests the potential for general toxicity (Koch et al., 2005; Badisa et al., 2009).

3.6.4. Histological examination of the tumor cells

3.6.4.1. HCT-116 cell line

The images revealed a continuous attached sheet exhibiting typical neoplastic characteristics in the untreated control group. At a concentration of 15.6 µg/mL, moderate lysis of cellularity was observed, characterized by empty spaces and prominent apoptosis. Furthermore, at 31.25 µg/mL, there was marked dissociation of cells and a loss of attachment between them, accompanied by numerous apoptotic bodies. Similarly, at 62.5 µg/mL, a decrease in cell density was noted, with increased spacing between apoptotic cells and cytoplasmic vacuolization. In contrast, at 125 µg/mL, all cellularity was lost, except for focal aggregations of small apoptotic cells. Finally, at concentrations of 250 and 500 µg/mL, there was a complete loss of cells due to destruction, with only a few apoptotic bodies remaining (Fig. 7).

3.6.4.2. Caco-2 cell line

The examination of images revealed significant changes in cell morphology and characteristics. In the untreated control group, the cells formed a continuous sheet of colorectal adenocarcinoma cells exhibiting typical neoplastic features. At a concentration of 15.6 µg/mL, mild gaps were observed between the cells, accompanied by the disruption of intercellular attachments and slight chromatin condensation. At 31.25 µg/mL, a marked disassociation of the majority of cells was noted, although large, atypical carcinoma cells remained present. Increasing the concentration to 62.5 µg/mL resulted in larger spaces between cells, significant chromatin condensation, and indications of apoptosis, with some clusters of cells still visible. At 125 µg/mL, each cell was isolated, displaying signs of cytoplasmic lysis and condensed chromatin. At 250 µg/mL, the cells were completely separated, and prominent signs of apoptosis were observed. Finally, at 500 µg/mL, only a few damaged cells and their debris were prominently visible. These findings indicate that treatment with AVeFHF induced significant alterations in the morphology and characteristics of Caco-2 cells, including disassociation, chromatin condensation, apoptosis, and cell debris. These observations suggest potential cytotoxic effects of AVeFHF on the Caco-2 cell line (Fig. 8).

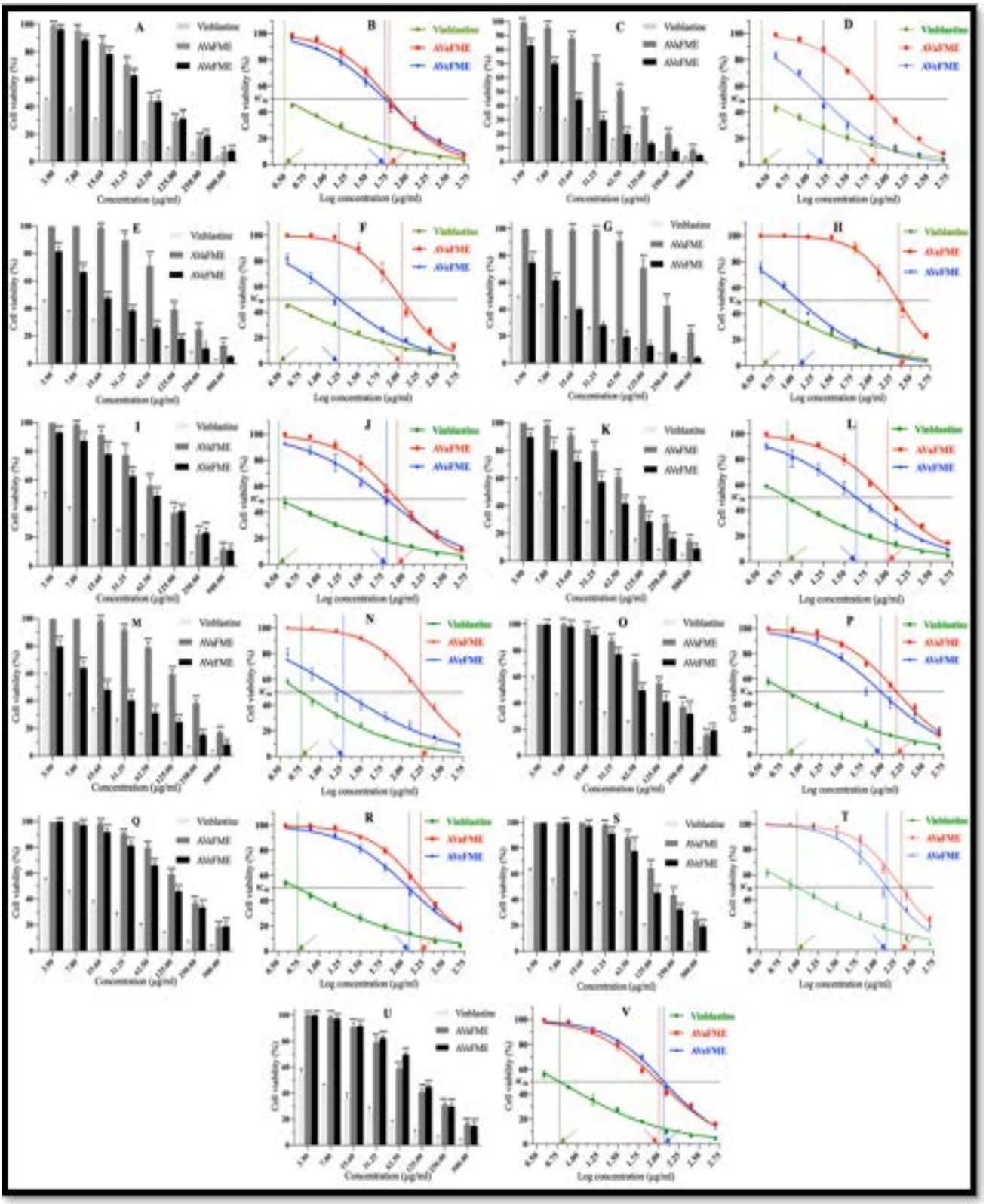

Fig. 4. Cytotoxic activity of AVeFME and AVaFME (3.9 to 500 µg/mL): (**A**) % of inhibition against HepG-2, (**B**) IC_{50} graph against HepG-2; (**C**) % of inhibition against HCT-116, (**D**) IC_{50} graph against HCT-116; (**E**) % of inhibition against Caco-2, (**F**) IC_{50} graph against Caco-2; (**G**) % of inhibition against A549, (**H**) IC_{50} graph against A549; (**I**) % of inhibition against MCF-7, (**J**) IC_{50} graph against MCF-7; (**K**) % of inhibition against PC-3, (**L**) IC_{50} graph against PC-3; (**M**) % of inhibition against RD, (**N**) IC_{50} graph against RD; (**O**) % of inhibition against HEP-2, (**P**) IC_{50} graph against HEP-2; (**Q**) % of inhibition against HELA, (**R**) IC_{50} graph against HELA; (**S**) % of inhibition against CHO-K1, (**T**) IC_{50} graph against CHO-K1; (**U**) % of inhibition against M-NFS-60, (**V**) IC_{50} graph against M-NFS-60 cell lines; $^{***}p$-value < 0.001, $^{**}p$-value < 0.01, $^{*}p$-value < 0.05 compared to standard. IC_{50} values were obtained from the log concentration response curve by GraphPad Prism 8 and the value is expressed as mean ± SD.

Table 6
IC_{50} values of AVeFME and AVaFME against different human cancer cell lines *vs.* vinblastine.

Tumor cell line	Mean of IC_{50} values (µg/mL) ± SD		
	Vinblastine	AVaFME	AVeFME
HepG-2	3.15 ± 1.71	60.53 ± 3.38***	53.88 ± 3.10***
HCT-116	2.61 ± 2.27	70.11 ± 2.49***	15.31 ± 3.56***
Caco-2	2.98 ± 1.95	10.60 ± 4.55***	17.58 ± 3.30***
A549	4.03 ± 2.19	221.60 ± 3.65***	12.02 ± 2.81***
MCF-7	3.29 ± 2.28	84.06 ± 3.94***	62.97 ± 3.60***
PC-3	6.90 ± 1.63	99.35 ± 2.91***	43.07 ± 3.75***
RD	5.79 ± 2.03	169.10 ± 2.22***	18.98 ± 4.41***
HEP-2	6.70 ± 2.55	147.60 ± 2.81***	94.33 ± 6.36***
HELA	5.49 ± 2.22	168.00 ± 1.84***	121.50 ± 3.11***
CHO-K1	9.49 ± 3.38	213.70 ± 3.22***	138.00 ± 5.13***
M-NFS-60	6.05 ± 2.43	101.40 ± 3.73***	116.60 ± 2.34***

IC_{50} (µg /mL): 1-10 (very strong), 11-25 (strong), 26-50 (moderate), 51-100 (weak), 100-200 (very weak), above 200 (non-cytotoxic); ***p-value < 0.001 compared to the standard drug.

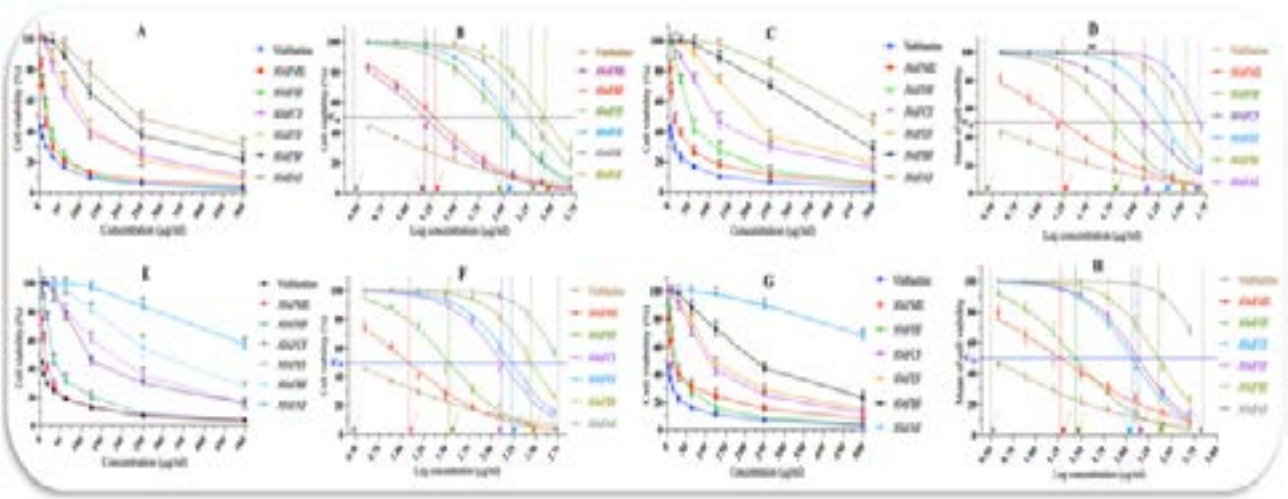

Fig. 5. Cytotoxicity activity of *A. vera* extract and its fractions (3.9 to 500 µg/mL) against HCT-116 (**A**, **B**), Caco-2 (**C**, **D**), A549 (**E**, **F**), and (**G**, **F**): (**A**, **C**, **E**, **G**) % of inhibition; (**B**, **D**, **F**, **H**) IC_{50} graph; ***p-value < 0.001, **p-value < 0.01 compared to standard; IC_{50} values obtained from the log concentration-response curve by GraphPad Prism 8 and the value is expressed as mean ± SD.

Table 7
IC_{50} values of *A. vera* different fractions against HCT-116, RD, Caco-2, and A549 cell lines *vs.* vinblastine.

Tumor cell line	Mean of IC_{50} values (µg/mL) ± SD						
	Vinblastine	AVeFME	AVeFHF	AVeFCF	AVeFEF	AVeFBF	AVeFAF
HCT-116	2.82 ± 2.20	15.31 ± 3.56*	19.33 ± 2.04***	96.94 ± 3.16***	109.70 ± 2.57***	193.10 ± 3.10***	271.80 ± 3.50***
Caco-2	2.63 ± 2.71	17.58 ± 3.30**	59.79 ± 3.75***	127.60 ± 3.19***	204.90 ± 2.57***	346.60 ± 2.22***	471.20 ± 1.05***
A549	2.82 ± 1.96	12.02 ± 2.81	34.14 ± 3.98***	132.60 ± 3.79***	168.90 ± 2.39***	282.10 ± 2.54***	>500
RD	3.15 ± 2.18	18.98 ± 4.41***	27.33 ± 3.33***	115.80 ± 2.69***	134.0 ± 2.80***	227.40 ± 2.70***	>500

AVeFME, *A. vera* flowers methanolic extract; AVeFHF, *A. vera* flowers *n*-hexane fraction; AVeFCF, *A. vera* flowers $CHCl_3$ fraction; AVeFEF, *A. vera* flowers EtOAc fraction; AVeFBF, *A. vera* flowers *n*-BuOH fraction; AVeFAF, *A. vera* flowers aqueous fraction; ***p-value < 0.001, **p-value < 0.01 compared to the reference drug.

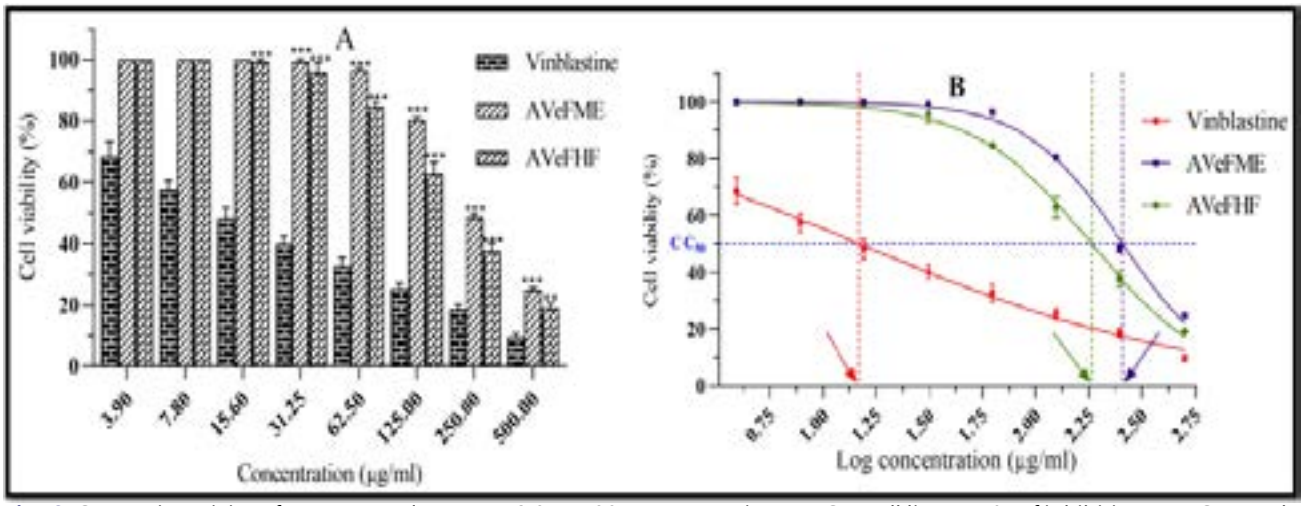

Fig. 6. Cytotoxic activity of AVeFME and AVeFHF (3.9 to 500 µg/mL) against MRC-5 cell line: (**A**) % of inhibition; (**B**) IC_{50} graph; $^{***}p$-value < 0.001, $^{**}p$-value < 0.01 compared to standard; CC_{50} values obtained from the log concentration-response curve by GraphPad Prism 8 and the value is expressed as mean ± SD.

Table 8

The selectivity index of AVeFME, AVeFHF, and standard on cancerous cell lines *vs.* a non-cancerous cell line.

Sample	MRC-5	HCT-116		Caco-2		A549		RD	
	CC_{50}	IC_{50}	SI	IC_{50}	SI	IC_{50}	SI	IC50	SI
AVeFME	257.30 ± 1.95***	15.31 ± 3.56*	16.81	17.58 ± 0.65**	14.64	12.02 ± 2.81	21.41	18.98 ± 4.41***	13.56
AVeFHF	183.00 ± 2.32***	19.33 ± 2.04***	9.47	59.79 ± 3.75***	3.06	34.14 ± 3.98***	5.36	27.33 ± 3.33***	6.7
Standard	14.81 ± 3.12	2.82 ± 2.20	5.25	2.63 ± 2.71	5.63	2.82 ± 1.96	5.25	3.15 ± 2.18	4.7

SI, selective index; AVeFME, *A. vera* flowers methanolic extract; AVeFHF, *A. vera* flowers hexane fraction; Standard, vinblastine; $^{***}p$-value < 0.001, $^{**}p$-value < 0.01, $^{*}p$-value < 0.05 compared to the reference drug.

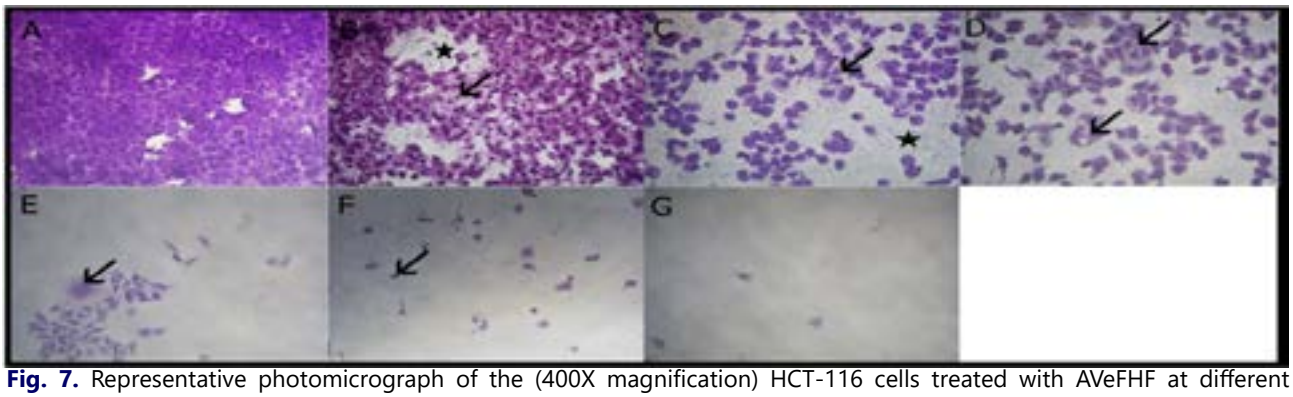

Fig. 7. Representative photomicrograph of the (400X magnification) HCT-116 cells treated with AVeFHF at different concentrations: **A)** non-treated control group. **B)** 15.6 µg/mL group. **C)** 31.25 µg/mL group. **D)** 62.5 µg/mL group. **E)** 125 µg/mL group. **F** and **G)** 250 and 500 µg/mL group.

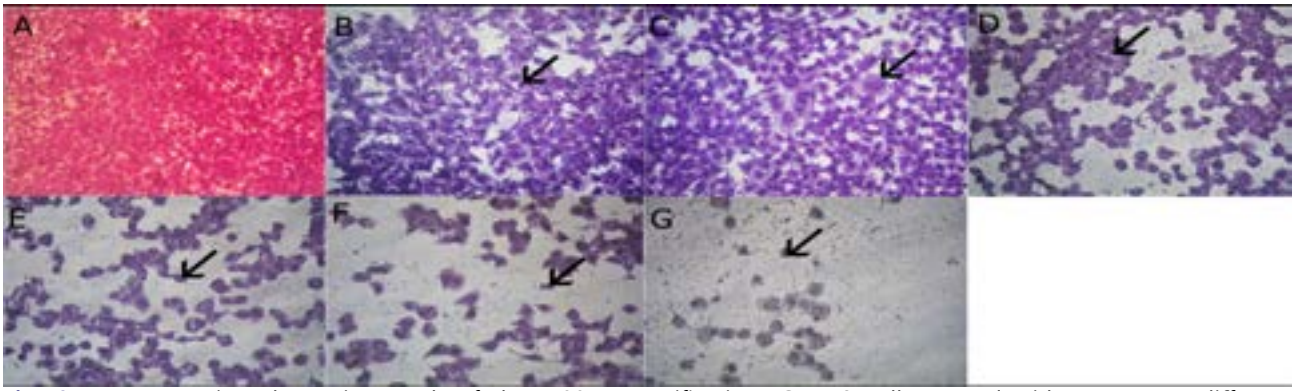

Fig. 8. Representative Photomicrograph of the (400X magnification) Caco-2 cells treated with AVeFHF at different concentrations: **A)** non-treated control group. **B)** 15.6 µg/mL group. **C)** 31.25 µg/mL group. **D)** 62.5 µg/mL group. **E)** 125 µg/mL group. **F)** 250 µg/mL group. **G)** 500 µg/mL group.

3.6.4.3. A549 cell line

The examination of images revealed distinct changes in cell morphology and characteristics. In the untreated control group, A549 cells exhibited a continuous sheet of adenocarcinoma human alveolar basal epithelial cells with typical neoplastic features. In the group treated with AVeFHF at a concentration of 15.6 µg/mL, a continuous sheet of cells was still observed, but with prominent atypical carcinoma cells. At a concentration of 31.25 µg/mL, empty areas adjacent to the associated cells became apparent, and numerous cells displayed signs of destruction and condensed chromatin. An increase in concentration to 62.5 µg/mL resulted in larger empty areas, more damaged cells, and the presence of marked apoptotic bodies. At concentrations of 125 and 250 µg/mL, the carcinoma cells were completely dissociated, and the chromatin appeared condensed. Apoptosis was also observed in these cells. Finally, at 500 µg/mL, no cells or remnants were detected, indicating complete cell lysis. These observations suggest that treatment with AVeFHF induced significant changes in the morphology and characteristics of A549 cells, including cellular dissociation, apoptosis, and cell lysis. These findings indicate the potential cytotoxic effects of AVeFHF on A549 cells (Fig. 9).

3.6.4.4. RD cell lines

Images of RD cells revealed a continuously attached sheet exhibiting typical neoplastic characteristics in the untreated control group. at 15.6 µg/mL, mild to moderate individual lysis of cellularity was observed, accompanied by clear destruction of cells and numerous dense chromatin structures, while maintaining attachment between cells. Furthermore, at 31.25 µg/mL, network-like cellular bands with atypical cells were noted in the RD cells. Individual empty spaces resulting from cell lysis, along with disappearing nuclei—except for numerous apoptotic bodies and vacuolated cytoplasm—were observed in the RD cells treated with AVeFHF at 62.5 and 125 µg/mL. The destruction of cells with apoptotic bodies was a common finding in RD cells treated with AVeFHF at the 250 µg/mL concentration. A complete disappearance of cells and their remnants was prominent in the RD cells treated with AVeFHF at the 500 µg/mL concentration (Fig. 10).

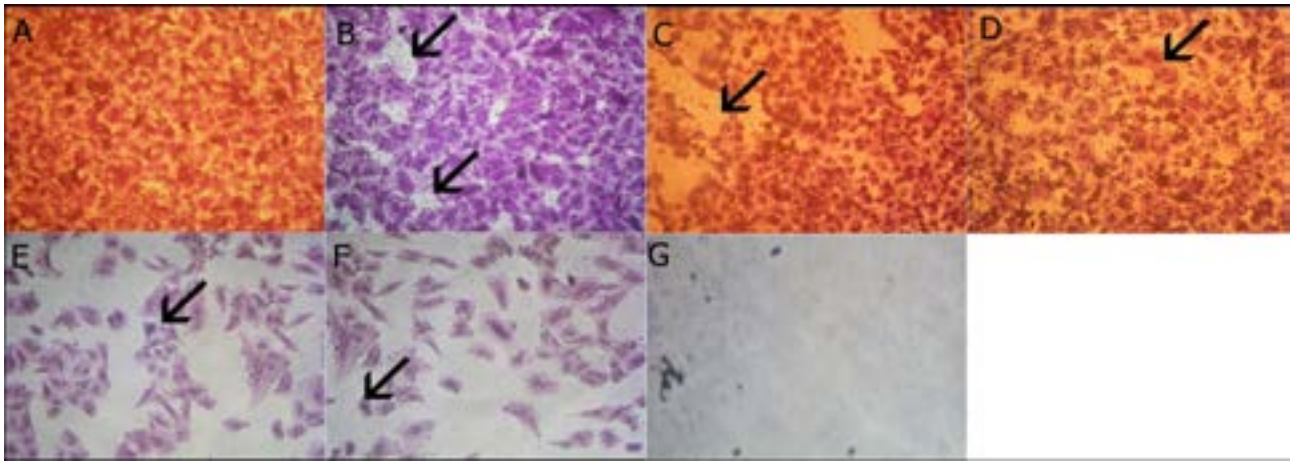

Fig. 9. Representative Photomicrograph of the (400X magnification) A549 cells treated with AVeFHF at different concentrations: **A)** non-treated control group. **B)** 15.6 µg/mL group. **C)** 31.25 µg/mL group. **D)** 62.5 µg/mL group. **E** and **F)** 125 and 250 µg/mL groups. **G)** 500 µg/mL group.

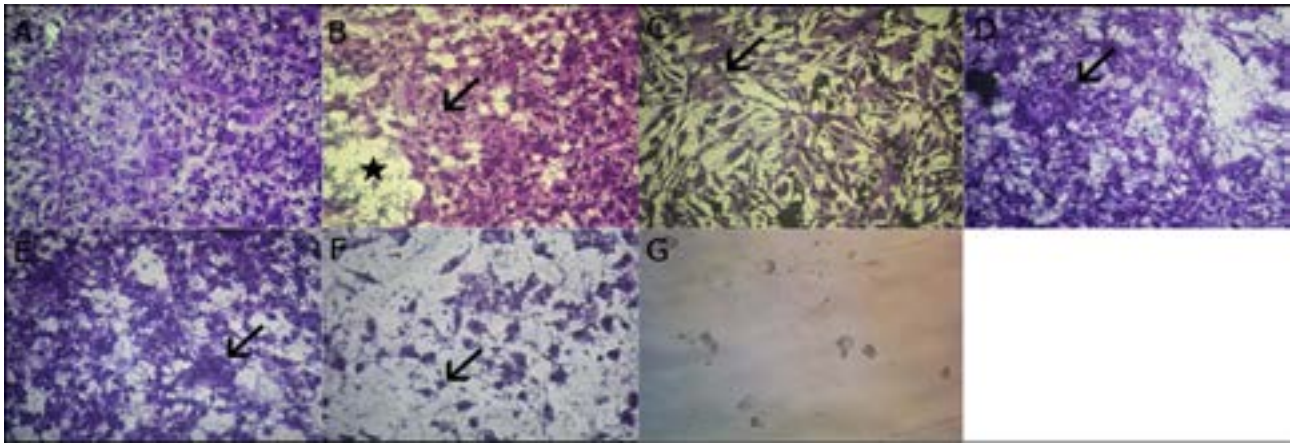

Fig. 10. Representative photomicrograph of the (400X magnification) RD cells treated with AVeFHF at different concentrations: **A)** non-treated control group. **B)** 15.6 µg/mL group. **C)** 31.25 µg/mL group. **D** and **E)** 62.5 and 125 µg/mL group. **F)** 250 µg/mL group. **G)** 500 µg/mL group.

3.6.5. Annexin V-FITC/PI dual staining and cell cycle analysis

To characterize the mode of cell death induced by AVeFME in HepG2 cells, we conducted a biparametric annexin V-FITC/propidium iodide (PI) cytofluorimetric analysis. The results indicated that the total percentage of apoptotic cells increased 22-fold after incubation with AVeFME (see Table 9 and Fig. 11A). Furthermore, cell cycle analysis was performed to detect potential changes in the cell cycle phases between control and treated cells. It was observed that AVeFME caused cell cycle arrest in the G1 phase, with a value of 59.01% (1.2-fold increase) compared to the control, as shown in Table 10 and Fig. 11B. Inducing apoptosis in cancer cells while minimizing side effects on normal cells is a remarkable and ideal factor in cancer treatment (Sain et al., 2012; Koff et al., 2015). Numerous studies have demonstrated that various constituents of A. vera can induce cell cycle arrest and apoptosis in cancer cells (Jeon et al., 2012; Suboj et al., 2012; Huang et al., 2013; Ismail et al., 2013).

Table 9
Effect of AVeFME on cell death process in HepG2 cells.

Compound	Total apoptosis (%)	Necrosis (%)
AVeFME	42.65	3.29
Control	1.94	1.43

AVeFME, *A. vera* flowers methanolic extract.

3.6.6. Molecular docking studies

Molecular docking provides insights into the various molecular interactions between AVFME and anticancer targets, including PI3K and EGFR. This analysis offers clues regarding the different mechanisms underlying the observed biological results.

3.6.6.1. Docking studies at PARP-1 (5DS3.pdb)

Inhibition of poly(ADP-ribose) polymerase-1 (PARP-1) is considered as a promising target for cancer therapy by hindering DNA repair (Torgovnick and Schumacher, 2015). Docking studies of GC-MS identified compounds showed high binding scores (–5.37 to –8.40 kcal/mol) compared to reference/co-crystalized ligand; olaparib (–8.07 kcal/mol) (Table 11). Docking results of selected compounds were summarized in (Table 12; Fig. 12).

3.6.6.2. Docking studies at EGFR (2RGP.pdb)

Epidermal Growth Factor Receptor (EGFR) is a trans-membrane glycoprotein with an extracellular epidermal growth factor binding domain and an intracellular tyrosine kinase domain that regulates signaling pathways to control cellular proliferation. Mutations can result in constitutive activation of signal transduction pathways, leading to cell proliferation or anti-apoptosis yielding more aggressive tumor phenotypes (Bethune et al., 2010).

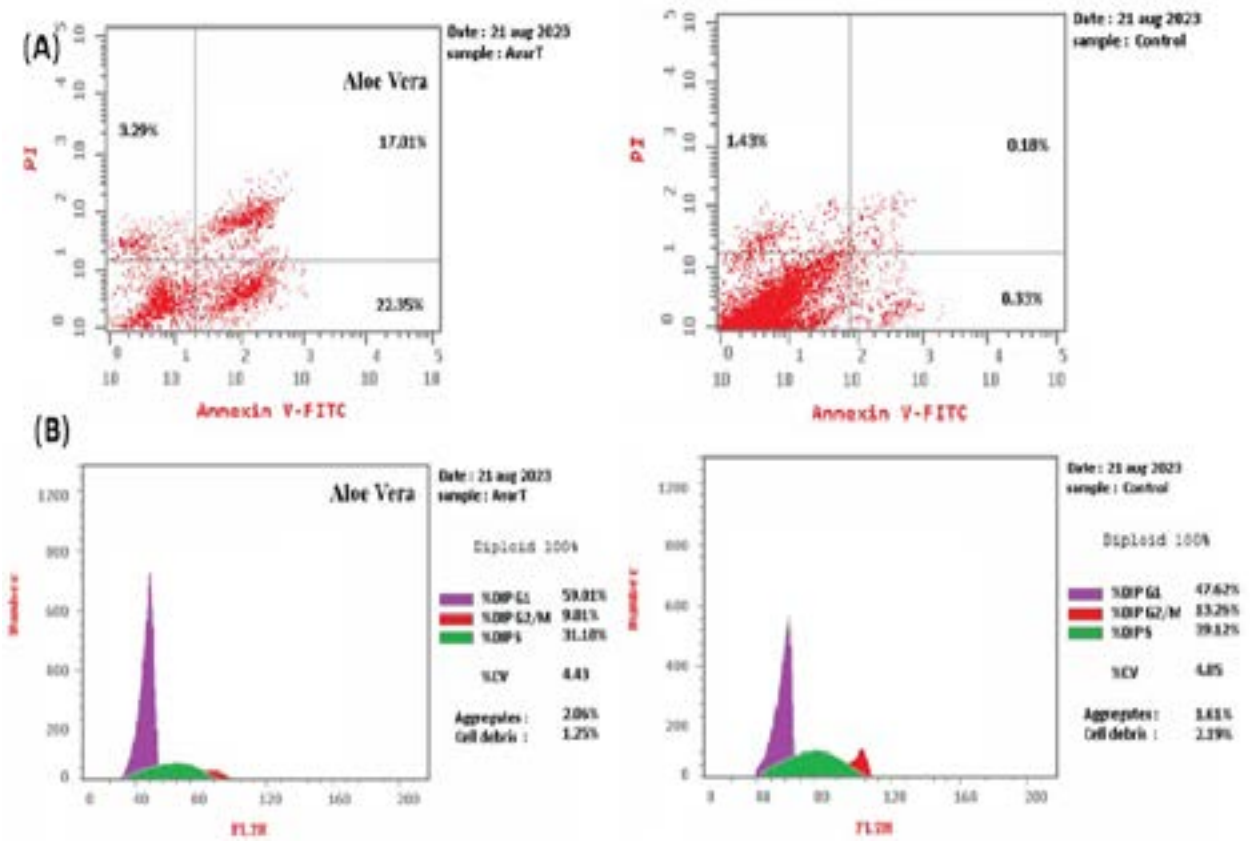

Fig. 11. (**A**) Effect of AVeFME on apoptosis induction in HepG2 cells relative to control using the annexin V-FITC/PI assay; (**B**) Cell cycle distribution analysis in HepG2 cells relative to control.

Table 10
The percentage of cells in each phase of the cell cycle for AVeFME-HepG2 and control-HepG2 cells.

Compound	%G0-G1	%S	%G2/M
AVeFME	59.01	31.18	9.81
Control	47.62	39.12	13.26

AVeFME, *A. vera* flowers methanolic extract.

Table 11
Binding scoring function (S) and rmsd values of the docked phenolic and flavonoid compounds, GC-MS identified compounds, and the co-crystallized ligands at PARP-1 (5DS3.pdb) and EGFR (2RGP.pdb).

Compound	PARP-1		EGFR	
	S (kcal/mol)	rmsd	S (kcal/mol)	rmsd
Benzyl benzoate	–5.37	1.89	–6.38	0.74
Myristic acid isopropyl ester	–6.94	1.15	–7.92	1.19
Methyl palmitate	–7.04	1.06	–8.32	0.91
n-Hexadecanoic acid	–6.87	1.61	–8.03	1.05
Hexadecanoic acid ethyl ester	–7.20	1.54	–8.27	1.68
9-Octadecenoic acid	–6.83	1.37	–8.04	1.48
9,12-Octadecadienoic acid methyl ester	–7.54	1.27	–8.61	1.8
9,12,15-Octadecatrienoic acid methyl ester	–7.11	1.89	–8.54	1.32
11-Octadecenoic acid methyl ester	–7.07	0.99	–8.23	1.11
Methyl stearate	–7.50	1.22	–9.10	1.06
Linoleic acid ethyl ester	–7.45	1.12	–8.44	1.13
9,12,15-Octadecatrienoic acid ethyl ester	–7.34	1.35	–8.72	1.53
Ethyl oleate	–7.41	1.2	–8.78	1.06
Stearic acid	–6.73	1.77	–8.08	1.85
Stearic acid ethyl ester	–7.76	1.54	–8.52	1.88
Glycidyl palmitate	–7.84	0.93	–8.45	1.38
Docosane	–7.74	1.65	–8.37	1.66
Bis(2-ethylhexyl) phthalate	–7.15	1.41	–9.21	1.39
Nonacosanol	–8.40	1.8	–9.46	1.81
Stigmast-5-en-3-ol	–7.66	1.44	–6.99	1.39
Octacosanol	–8.06	1.96	–9.20	1.56
Campesterol	–7.47	1.1	–7.06	1.97
9,19-Cycloergost-24(28)-en-3-ol, 4,14-dimethyl acetate	–7.62	1.74	–5.91	1.8
Sinapic acid	–5.54	0.95	–5.65	0.96
Quercitrin	–6.00	1.26	–6.07	0.88
Kaempferol	–6.03	1.9	–6.46	1.15
Apigenin	–5.92	1.18	–5.89	1.83
Gallic acid	–4.87	0.77	–5.34	0.78
Catechin	–5.83	1.44	–6.26	1.64
Epicatechin	–5.81	1.54	–6.26	1.64
Syringic acid	–5.10	0.73	–5.34	0.85
Chlorogenic acid	–6.22	1.79	–7.20	1.52
Gentisic acid	–4.76	0.97	–5.28	1.72
Caffeic acid	–5.04	1.49	–5.14	1.26
Coumaric acid	–4.80	1.05	–4.91	1.87

Table 11
Continued

Compound	PARP-1		EGFR	
	S (kcal/mol)	rmsd	S (kcal/mol)	rmsd
Rutin	–8.77	1.6	–8.06	1.07
Myricetin	–5.96	1.33	–6.28	0.69
Aloesin or aloeresin B	–6.92	1.57	–7.88	0.76
Aloe emodin diglucoside	–8.48	1.72	–7.85	1.8
Isoquercitrin	–7.63	1.59	–7.78	1.16
Kaempferol-3-*O*-hexosyl-*O*-pentoside	–8.42	1.25	–8.74	1.65
Luteolin-8-C-glucoside (orientin)	–7.34	1.13	–8.93	1.23
Feruloylquinic acid	–6.38	2.21	–8.09	1.54
10-Hydroxyaloin A	–7.27	1.21	–6.30	1.6
Isovitexin	–6.93	0.97	–7.74	1.08
Chrysoeriol-7-*O*-glucuronide	–7.80	1.41	–8.96	1.41
Aloin A	–6.75	1.43	–6.48	1.86
Isoaloeresin D	–8.81	1.93	–8.98	1.98
6′-Malonylnataloin	–6.79	1.75	–8.10	1.78
Aloe emodin-8-*O*-glucoside	–6.58	1.94	–7.43	1.69
Eupatorin	–8.20	1.72	–6.75	1.35
Stigmast-4-en-3-one	–7.48	1.1	–6.57	1.84
Co-crystallized ligand; olaparib	–8.07	1.62	--------	-------
Co-crystallized ligand; HYZ	-------	-------	–8.70	1.91

PARP-1, Poly(ADP-ribose) polymerase-1; EGFR, Epidermal growth factor receptor.

Table 12
Hexadecanoic acid ethyl ester, glycidyl palmitate, bis(2-ethylhexyl) phthalate, stigmast-5-en-3-ol, stigmast-4-en-3-one, 9,12-octadecadienoic acid methyl ester, rutin, kaempferol-3-*O*-hexosyl-*O*-pentoside, and isoaloeresin D binding poses at PARP-1 (PDB ID: 5DS3) and EGFR (2RGP.pdb) binding sites.

Compound	Ligands and PARP-1 interactions		Ligands and EGFR interactions	
	HB interactions, No. of interactions	Hydrophobic interactions	HB interactions, No. of interactions	Hydrophobic interactions
Hexadecanoic acid ethyl ester	His862, Gly863, Ser904 (4HB)	Tyr907 (2)	Met766, Cyc797 (6HB)	Leu788 (1)
Glycidyl palmitate	Gly863, Ser904 (2HB)	His862, Tyr896 (2)	Lys745, Met766, Cyc797, Thr854, Asp855 (5HB)	Leu788, Leu718, Val720 (3)
Bis(2-ethylhexyl) phthalate	His862, Ser864 (2HB)	Tyr907 (3)	Met766, Cyc797 (2HB)	------
Stigmast-4-en-3-one	Arg878 (2HB)	His862, Tyr889, Tyr907 (4)	Cys797, Asp855 (3HB)	Leu844
Rutin	Lys903, Tyr907 (2HB)	Ile872, Tyr896 (3)	Leu718, Ala743, Lys745, Cys797 (4HB)	Gly796, Leu844 (2)
Kaempferol-3-O-hexosyl-O-pentoside	Gly888 (1HB)	Tyr896, Lys903 (2)	Lys745, Cys797 (3HB)	Gly796 (1)
Isoaloeresin D	Tyr907, Gly863 (2HB)	Arg878 (1)	Met766, Lys797, Asp855 (3HB)	Leu718, Cys797 (4)
Stigmast-5-en-3-ol	His862, Arg878 (3HB)	Tyr907 (3)	------	------
9,12-Octadecadienoic acid methyl ester	------	------	Met766, Cyc797 and Asp855 (4HB)	------

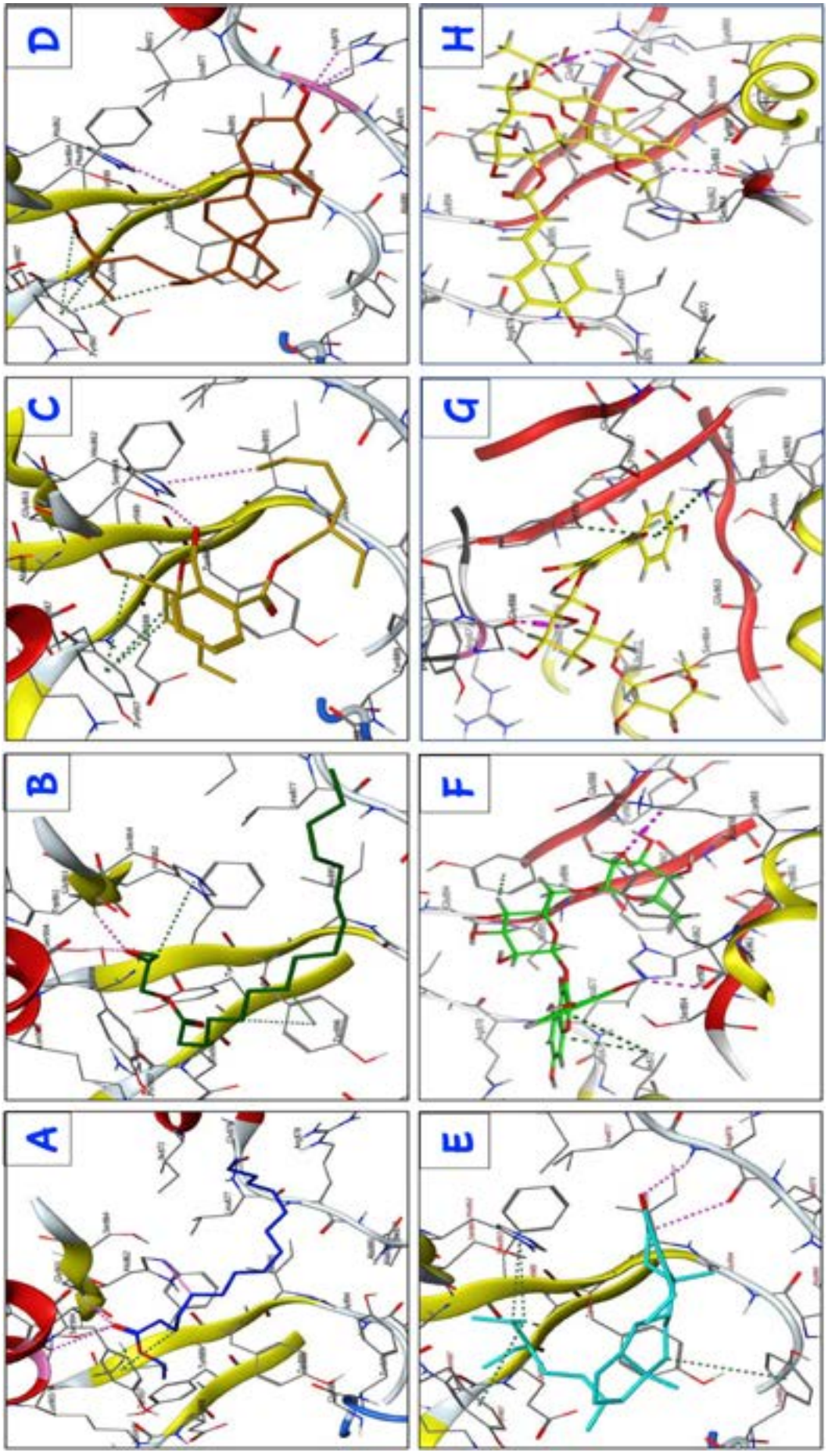

Fig. 12. Binding poses of Hexadecanoic acid ethyl ester **(A)**, glycidyl palmitate **(B)**, bis(2-ethylhexyl) phthalate **(C)**, stigmast-5-en-3-ol **(D)**, stigmast-4-en-3-one **(E)**, rutin **(F)**, kaempferol-3-*O*-hexosyl-*O*-pentoside **(G)**, Isoaloeresin D **(H)** at PARP-1 (PDB ID: 5DS3) binding site.

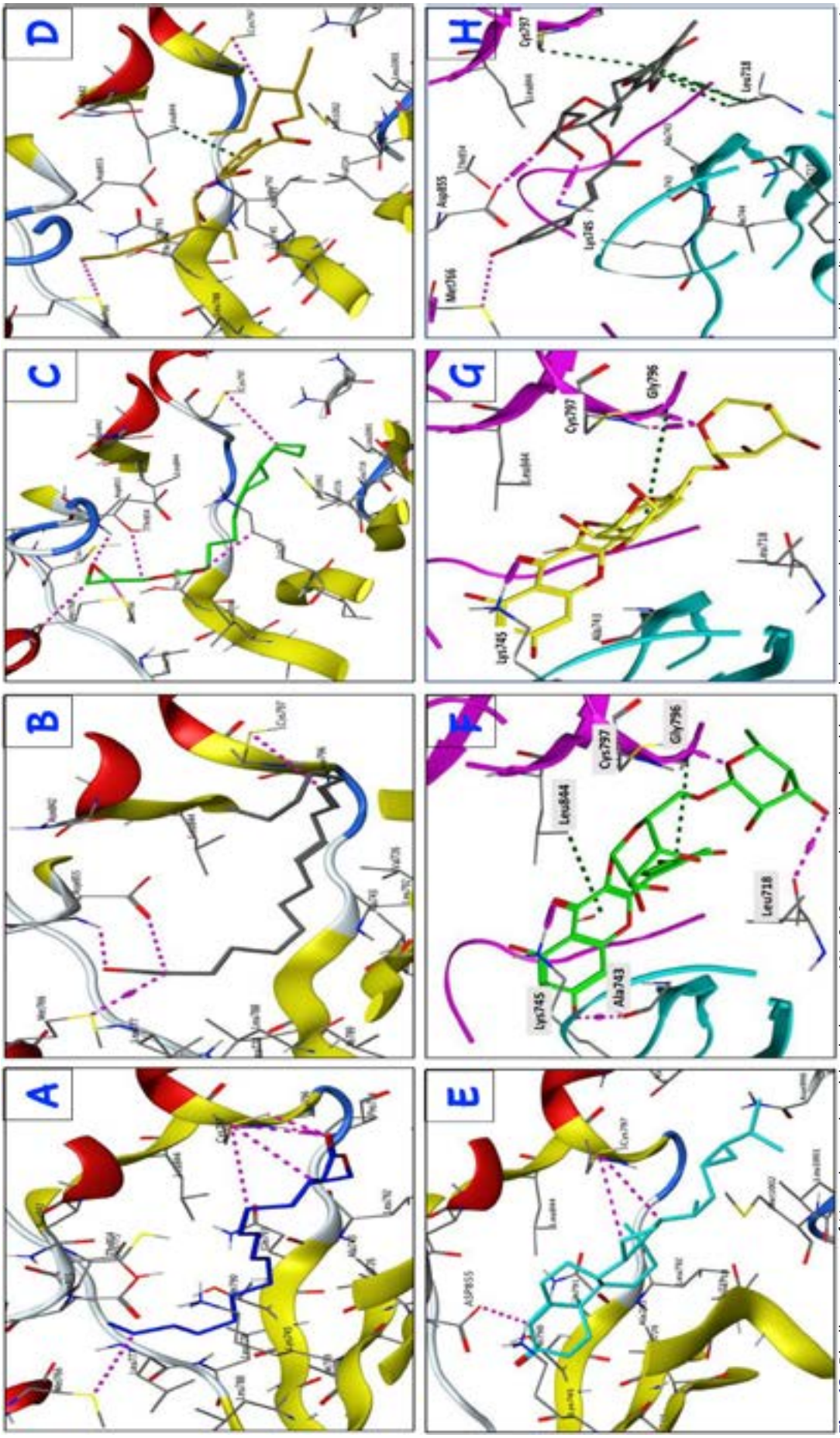

Fig. 13. Binding poses of Hexadecanoic acid ethyl ester (**A**), 9,12-octadecadienoic acid methyl ester (**B**), glycidyl palmitate (**C**), bis(2-ethylhexyl) phthalate (**D**), and stigmast-4-en-3-one (**E**) at EGFR (2RGP.pdb) binding site.

Understanding molecular interactions of selected hexane fraction molecules and EGFR (2RGP.pdb) was gained using *in silico* studies. Results of the docked molecules revealed a binding score range from –5.91 to –9.46 kcal/mol as well as –8.70 kcal/mol for the redocked co-crystalized ligand HYZ (Table 11). The docking results of selected molecules were summarized in Table 12 and Fig. 13. It was shown that the results of docking data were inconsistent with the obtained anticancer data which is in cope with literature; fatty acid and their ester (Jóźwiak et al., 2020; Breeta et al., 2021; Yamagata et al., 2021), phytosterol (stigmasterol, Stigmast-5-en-3-ol, ... etc) (Awad and Fink, 2000; Shahzad et al., 2017; Fernando et al., 2018), polyphenolics and flavonoids (Harlev et al., 2012; Imran et al., 2019; Pandey et al., 2021).

4. Concluding remarks

This research study aimed to investigate the potential activities of selected *Aloe* species that possess important biological properties, including cytotoxic and antioxidant activities. AVeFME showed high efficacy against HCT-116, Caco-2, A-549, and RD cell lines, while AVaFME did not exhibit any promising effects on the tested cell lines. The cytotoxic activity of AVeFME may be attributed to its active components, such as phenolic compounds and flavonoids. The histological examination of the treated cell lines at different concentrations of AVeFME revealed notable morphological changes, similar to those observed in the apoptotic mechanism of action. The *in silico* study provided insights into the rational binding modes of PARP-1 and EGFR enzymes with the identified compounds. Further research is needed to elucidate the precise mechanisms of action and to validate these findings *in vivo* and in clinical trials.

Author contribution statement

Ama Mohsan Mohammed Al-wajih: Writing-original draft, plant collection and phytochemical study, and biological analysis. Amina El-shaibany: Conceptualization, phytochemical study, review and editing. Mahmoud Mahyoob Alburhyi: Biological and histological analysis; Ahmed S. Abdelkhalek: Writing-original draft, molecular docking study, review and editing. Mahmoud M. Elaasser: Biological analysis. Ali E. Raslan: Phytochemical study, statistical analysis, writing - original draft, review and editing.

Conflict of interest

The authors declare that there is no conflict of interest.

References

Abdollahi-Ghehi, H., Sonboli, A., Ebrahimi, S.N., Esmaeili, M.A., Mirjalili, M.H., 2019. Triterpenic acid content and cytotoxicity of some *Salvia* species from Iran. Nat. Prod. Commun. 14(5), 1-10.

Aberoumandi, S.M., Mohammadhosseini, M., Abasi, E., Saghati, S., Nikzamir, N., Akbarzadeh, A., Panahi, Y., Davaran, S., 2017. An update on applications of nanostructured drug delivery systems in cancer therapy: A review. Artif. Cells Nanomed. Biotechnol. 45(6), 1058-1068.

Al-Fatimi, M., 2023. Ethnopharmacological survey of endemic plants used in ethnomedicinal knowledge of Soqotra Island. J. Ethnopharmacol. 304, 116033.

Al-Hakami, I.A., El-Shaibany, A., Al-Mahbashi, H., Abdelkhalek, A.S., Elaasser, M.M., Raslan, A.E., 2024. GC-MS profiling and evaluation of acute oral toxicity, anti-tumour, antimicrobial and antioxidant activities of Croton socotranus Balf.f. aerial parts: *In-vitro*, *in-vivo* and *in-silico* studies. Nat. Prod. Res. 38(24), 4307-4316.

Amin, B.H., Ahmed, H.Y., Abd El-Aziz, M.M., 2018. *In vitro* anticancer activity of fungal secondary metabolites of *Stemphylium lycopersici*. N. Egypt. J. Microbiol. 50, 80-97.

Arputhaswamy, V., Rajkumar, V., Thomas, N.M., Sathasivam, V., Muthukrishnan, A., Packiaraj, G., 2024. Biochemical profiling and anticancer properties of brown seaweed *Dictyota dichotoma* (Hudson.) J.V.Lamouroux. Trends Phytochem. Res. 8(4), 261-276.

Awad, A.B., Fink, C.S., 2000. Phytosterols as anticancer dietary components: Evidence and mechanism of action. J. Nutr. 130(9), 2127-2130.

Badisa, R.B., Darling-Reed, S.F., Joseph, P., Cooperwood, J.S., Latinwo, L.M., Goodman, C.B., 2009. Selective cytotoxic activities of two novel synthetic drugs on human breast carcinoma MCF-7 cells. Anticancer Res. 29(8), 2993-2996.

Bailly, C., 2021. Anticancer butanolides and lignans from the Makko tree, *Machilus thunbergii* Siebold & Zucc. (Lauraceae). A review. Trends Phytochem. Res. 5(3), 136-147.

Bello, I., Bakkouri, A.S., Tabana, Y.M., Al-Hindi, B., Al-Mansoub, M.A., Mahmud, R., Asmawi, M.Z., 2016. Acute and sub-acute toxicity evaluation of the methanolic extract of *Alstonia scholaris* stem bark. Med. Sci. 4(1), 4.

Bethune, G., Bethune, D., Ridgway, N., Xu, Z., 2010. Epidermal growth factor receptor (EGFR) in lung cancer: An overview and update. J. Thorac. Dis. 2(1), 48-51.

Breeta, R.D.I.E., Grace, V.M.B., Wilson, D.D., 2021. Methyl Palmitate—A suitable adjuvant for sorafenib therapy to reduce *in vivo* toxicity and to enhance anti-cancer effects on hepatocellular carcinoma cells. Basic Clin. Pharmacol. Toxicol. 128(3), 366-378.

Chan, L.L., George, S., Ahmad, I., Gosangari, S.L., Abbasi, A., Cunningham, B.T., Watkin, K.L., 2011. Cytotoxicity effects of *Amoora rohituka* and chittagonga on breast and pancreatic cancer cells. Evid. Based Complement. Alternat. Med. 2011, 860605.

Chen, R., Zhang, J., Hu, Y., Wang, S., Chen, M., Wang, Y., 2014. Potential antineoplastic effects of aloe-emodin: A comprehensive review. Am. J. Chin. Med. 42(02), 275-288.

Dekdouk, N., Ameddah, S., Bensouici, C., Ibtissem, M., Ahmed, M., Martel, F., 2024. Antioxidant properties and anticancer activity of Olea europaea L. olive and Ficus carica fruit extracts against pancreatic cancer cell lines. Trends Phytochem. Res. 8(2), 80-92.

Dixit, S., Ali, H., 2010. Anticancer activity of medicinal plant extract-A review. J. Chem. Chem. Sci. 1(1), 79-85.

Elkomy, N.M.I.M., El-Shaibany, A., Elnagar, G.M., Abdelkhalek, A.S., Al-Mahbashi, H., Elaasser, M.M., Raweh, S.M., Aldiyarbi, M.A., Raslan, A.E., 2023. Evaluation of acute oral toxicity, anti-diabetic and antioxidant effects of *Aloe vera* flowers extract. J. Ethnopharmacol. 309, 116310.

Elsanhoty, R.M., Soliman, M.S., Khidr, Y.A., Hassan,

G.O., Hassan, A.R., Aladhadh, M., Abdella, A., 2022. Pharmacological activities and characterization of phenolic and flavonoid compounds in *Solenostemma argel* extract. Molecules 27(23), 8118.
Fathi Karkan, S., Mohammadhosseini, M., Panahi, Y., Milani, M., Zarghami, N., Akbarzadeh, A., Abasi, E., Hosseini, A., Davaran, S., 2017. Magnetic nanoparticles in cancer diagnosis and treatment: A review. Artif. Cells Nanomed. Biotechnol. 45(1), 1-5.
Fernando, I.S., Sanjeewa, K.A., Ann, Y.-S., Ko, C.-i., Lee, S.-H., Lee, W.W., Jeon, Y.-J., 2018. Apoptotic and antiproliferative effects of Stigmast-5-en-3-ol from Dendronephthya gigantea on human leukemia HL-60 and human breast cancer MCF-7 cells. Toxicol. In Vitro 52, 297-305.
Geran, R., Greenberg, N., Macdonald, M., Schumacher, A., 1972. Protocols for screening chemical agents and natural products against animal tumors and other biological systems. Cancer Chemother. Rep. 3, 59-61.
Goldstein, M.S., 2003. Complementary and alternative medicine: Its emerging role in oncology. J. Psychosoc. Oncol. 21(2), 1-21.
Harlev, E., Nevo, E., Lansky, E.P., Ofir, R., Bishayee, A., 2012. Anticancer potential of aloes: Antioxidant, antiproliferative, and immunostimulatory attributes. Planta Med. 78(09), 843-852.
Huang, P.H., Huang, C.Y., Chen, M.C., Lee, Y.T., Yue, C.H., Wang, H.Y., Lin, H., 2013. Emodin and aloe-emodin suppress breast cancer cell proliferation through ERα inhibition. Evid. Based Complement. Alternat. Med. 2013, 376123.
Hussain, A., Sharma, C., Saniyah, K., Kruti, S., Shafiul, H., 2015. *Aloe vera* inhibits proliferation of human breast and cervical cancer cells and acts synergistically with cisplatin. Asian Pac. J. Cancer Prev. 16(7), 2939-2946.
Imran, M., Salehi, B., Sharifi-Rad, J., Aslam Gondal, T., Saeed, F., Imran, A., Shahbaz, M., Tsouh Fokou, P.V., Umair Arshad, M., Khan, H., 2019. Kaempferol: A key emphasis to its anticancer potential. Molecules 24(12), 2277.
Ismail, S., Haris, K., Abdul Ghani, A.R.I., Abdullah, J.M., Johan, M.F., Mohamed Yusoff, A.A., 2013. Enhanced induction of cell cycle arrest and apoptosis via the mitochondrial membrane potential disruption in human U87 malignant glioma cells by aloe emodin. J. Asian Nat. Prod. Res. 15(9), 1003-1012.
Jeon, W., Jeon, Y.K., Nam, M.J., 2012. Apoptosis by aloe-emodin is mediated through down-regulation of calpain-2 and ubiquitin-protein ligase E3A in human hepatoma Huh-7 cells. Cell Biol. Int. 36(2), 163-167.
Jóźwiak, M., Filipowska, A., Fiorino, F., Struga, M., 2020. Anticancer activities of fatty acids and their heterocyclic derivatives. Eur. J. Pharmacol. 871, 172937.
Keyhanian, S., Stahl-Biskup, E., 2007. Phenolic constituents in dried flowers of *Aloe vera* (Aloe barbadensis) and their in vitro antioxidative capacity. Planta Med. 73(06), 599-602.
Koch, A., Tamez, P., Pezzuto, J., Soejarto, D., 2005. Evaluation of plants used for antimalarial treatment by the Maasai of Kenya. J. Ethnopharmacol. 101(1-3), 95-99.
Koff, J.L., Ramachandiran, S., Bernal-Mizrachi, L., 2015. A time to kill: Targeting apoptosis in cancer. Int. J. Mol. Sci. 16(2), 2942-2955.
Konaka, H., Egawa, S., Saito, S., Yorozu, A., Takahashi, H., Miyakoda, K., Fukushima, M., Dokiya, T., Yamanaka, H., Stone, N.N., 2012. Tri-Modality therapy with I-125 brachytherapy, external beam radiation therapy, and short-or long-term hormone therapy for high-risk localized prostate cancer (TRIP): Study protocol for a phase III, multicenter, randomized, controlled trial. BMC Cancer 12(1), 1-10.
Lissoni, P., Rovelli, F., Brivio, F., Zago, R., Colciago, M., Messina, G., Mora, A., Porro, G., 2009. A randomized study of chemotherapy versus biochemotherapy with chemotherapy plus Aloe arborescens in patients with metastatic cancer. In Vivo 23(1), 171-175.
Liu, K., Park, C., Li, S., Lee, K.W., Liu, H., He, L., Soung, N.K., Ahn, J.S., Bode, A.M., Dong, Z., 2012. Aloe-emodin suppresses prostate cancer by targeting the mTOR complex 2. Carcinogenesis 33(7), 1406-1411.
López, A., De Tangil, M.S., Vega-Orellana, O., Ramírez, A.S., Rico, M., 2013. Phenolic constituents, antioxidant and preliminary antimycoplasmic activities of leaf skin and flowers of *Aloe vera* (L.) Burm. f.(syn. A. barbadensis Mill.) from the Canary Islands (Spain). Molecules 18(5), 4942-4954.
Mahdavi, B., Mohammadhosseini, M., 2022. Antioxidant, antimicrobial and anti-prostate cancer activity of the extracts from different parts of *Etlingera velutina* (Ridl.) R. M. Sm (Zingiberaceae). Trends Phytochem. Res. 6(4), 353-362.
Majumder, R., Das, C.K., Mandal, M., 2019. Lead bioactive compounds of *Aloe vera* as potential anticancer agent. Pharmacol. Res. 148, 104416.
Majumder, R., Parida, P., Paul, S., Basak, P., 2020. *In vitro* and *in silico* study of *Aloe vera* leaf extract against human breast cancer. Nat. Prod. Res. 34(16), 2363-2366.
Mishra, K., Ojha, H., Chaudhury, N.K., 2012. Estimation of antiradical properties of antioxidants using DPPH assay: A critical review and results. Food Chem. 130(4), 1036-1043.
Mohadjerani, M., Asadollahi, S., 2019. Veronica cristagalli Steven and Veronica persica Poir. as anticancer and antioxidant plants in-vitro. Trends Phytochem. Res. 3(1), 61-66.
Motta, L.B., Furlan, C.M., Santos, D.Y., Salatino, M.L., Duarte-Almeida, J.M., Negri, G., Carvalho, J.E.d., Ruiz, A.L.T., Cordeiro, I., Salatino, A., 2011. Constituents and antiproliferative activity of extracts from leaves of Croton macrobothrys. Rev. Bras. Farmacogn. 21, 972-977.
Mukherjee, P.K., Nema, N.K., Maity, N., Mukherjee, K., Harwansh, R.K., 2014. Phytochemical and therapeutic profile of *Aloe vera*. J. Nat. Remedies 14(1), 1-26.
Newman, D.J., Cragg, G.M., Snader, K.M., 2003. Natural products as sources of new drugs over the period 1981-2002. J. Nat. Prod. 66(7), 1022-1037.
Pandey, P., Khan, F., Qari, H.A., Oves, M., 2021. Rutin (Bioflavonoid) as cell signaling pathway modulator: Prospects in treatment and chemoprevention. Pharmaceuticals 14(11), 1069.
Quispe, C., Villalobos, M., Bórquez, J., Simirgiotis, M., 2018. Chemical composition and antioxidant activity of *Aloe vera* from the Pica Oasis (Tarapacá, Chile) by UHPLC-Q/Orbitrap/MS/MS. J. Chem. 2018(1), 6123850.
Reddy, L., Odhav, B., Bhoola, K., 2003. Natural products for cancer prevention: A global perspective. Pharmacol. Ther. 99(1), 1-13.
Rehman, M.H.U., Saleem, U., Ahmad, B., Rashid, M., 2022. Phytochemical and toxicological evaluation of Zephyranthes citrina. Front. Pharmacol. 13, 1007310.
Sain, R.K., Chouhan, R., Bagri, L.P., Bajpa, A., 2012. Strategies of targeting tumors and cancers. J. Cancer Res. Updates.

1(1), 129-152.
Sak, K., 2014. Cytotoxicity of dietary flavonoids on different human cancer types. Pharmacogn. Rev. 8(16), 122-146.
Shahzad, N., Khan, W., Shadab, M., Ali, A., Saluja, S.S., Sharma, S., Al-Allaf, F.A., Abduljaleel, Z., Ibrahim, I.A.A., Abdel-Wahab, A.F., 2017. Phytosterols as a natural anticancer agent: Current status and future perspective. Biomed. Pharmacother. 88, 786-794.
Suboj, P., Babykutty, S., Srinivas, P., Gopala, S., 2012. Aloe emodin induces G2/M cell cycle arrest and apoptosis via activation of caspase-6 in human colon cancer cells. Pharmacology 89(1-2), 91-98.
Tong, X., Li, M., Li, D., Lao, C., Chen, J., Xu, W., Du, J., Zhang, M., Yang, X., Li, J., 2021. *Aloe vera* gel extract: Safety evaluation for acute and chronic oral administration in Sprague-Dawley rats and anticancer activity in breast and lung cancer cells. J. Ethnopharmacol. 280, 114434.
Torgovnick, A., Schumacher, B., 2015. DNA repair mechanisms in cancer development and therapy. Front. Genet. 6, 157.
Yamagata, K., Uzu, E., Yoshigai, Y., Kato, C., Tagami, M., 2021. Oleic acid and oleoylethanolamide decrease interferon-γ-induced expression of PD-L1 and induce apoptosis in human lung carcinoma cells. Eur. J. Pharmacol. 903, 174116.
Zorzanelli, B.C., de Queiroz, L.N., Santos, R.M., Menezes, L.M., Gomes, F.C., Ferreira, V.F., C da Silva, F.d., Robbs, B.K., 2018. Potential cytotoxic and selective effect of new benzo [b] xanthenes against oral squamous cell carcinoma. Future Med. Chem. 10(10), 1141-1157.